

Analysis of Cause-Effect Inference via Regression Errors

Patrick Blöbaum¹, Dominik Janzing², Takashi Washio¹, Shohei Shimizu^{1,3}, and Bernhard Schölkopf²

¹Osaka University, Japan

²MPI for Intelligent Systems, Tübingen, Germany

³Shiga University, Japan

Abstract

We address the problem of inferring the causal relation between two variables by comparing the least-squares errors of the predictions in both possible causal directions. Under the assumption of an independence between the function relating cause and effect, the conditional noise distribution, and the distribution of the cause, we show that the errors are smaller in causal direction if both variables are equally scaled and the causal relation is close to deterministic. Based on this, we provide an easily applicable algorithm that only requires a regression in both possible causal directions and a comparison of the errors. The performance of the algorithm is compared with different related causal inference methods in various artificial and real-world data sets.

1 Introduction

Causal inference [2, 3] is becoming an increasingly popular topic in machine learning, since the results are often not only from interest in predicting the result of

This is an extended version of the AISTATS 2018 paper [1]. Compared to [1], this work mainly differs by providing detailed mathematical proofs and further extensive experiments.

potential interventions, but also in general statistical and machine learning applications [4]. In particular, the identification of the causal relation between only two observed variables is a challenging task [5, 6, 7, 8, 9, 10, 11, 12, 13, 14, 15, 16]. As regards the present work, we address this bivariate setting, where one variable is the cause and the other variable is the effect. That is, given observed data X, Y that are drawn from a joint distribution $p_{X,Y}$, we are interested in inferring whether X caused Y or Y caused X . For instance, is a certain change of the physical state of a patient a symptom or a cause of a certain disease? If we are not able to observe the effect of an intervention on one of the variables, the identification of the correct causal relation generally relies on the exploitation of statistical asymmetries between cause and effect [2, 3, 10, 14, 7]. Conventional approaches to causal inference rely on conditional independences and therefore require at least three observed variables. Given the observed pattern of conditional dependences and independences, one infers a class of directed acyclic graphs (DAGs) that are compatible with the respective pattern (subject to Markov condition and faithfulness assumption [2, 3]). Whenever there are causal arrows that are common to all DAGs in the class, conditional (in)dependences yield definite statements about causal directions.

In case of bivariate data, however, we rely on those types of asymmetries between cause and effect that are already apparent in the bivariate distribution alone. One kind of asymmetry is given by restricting the structural equations relating cause and effect to a certain function class: For linear relations with non-Gaussian independent noise, the linear non-Gaussian acyclic model (LiNGAM) [7] guarantees to identify the correct causal direction. For nonlinear relations, the additive noise model (ANM) [10] and its generalization to post-nonlinear models (PNL) [9] identify the causal direction by assuming an independence between cause and noise, where, apart from some exceptions such as bivariate Gaussian, a model can only be fit in the correct causal direction such that the input is independent of the residual.

Further recent approaches for the bivariate scenario are based on an *informal* independence assumption stating that the distribution of the cause, denoted by p_C contains no information about the conditional distribution of the effect, given the cause, denoted by $p_{E|C}$. Here, the formalization of ‘no information’ is a challenging task. For the purpose of foundational insights (rather than for practical purposes), [17] and [18] formalize the idea via *algorithmic information* and postulate that knowing p_C does not enable a shorter description of $p_{E|C}$ and vice versa. The information-geometric approach for causal inference (IGCI) [14] is inspired by the independence assumption and is able to infer the causal direction

in deterministic nonlinear relationships subject to a certain independence condition between the slope of the function and the distribution of the cause. A related but different independence assumption is also used by a technique called unsupervised inverse regression (CURE) [15], where the idea is to estimate a prediction model of both possible causal directions in an unsupervised manner, i.e. only the input data is used for the training of the prediction models. According to the above independence assumption, the effect data may contain information about the relation between cause and effect that can be employed for predicting the cause from the effect, but the cause data alone does not contain any information that helps the prediction of the effect from the cause (as hypothesized in [19]). Accordingly, the unsupervised regression model in the true causal direction should be less accurate than the prediction model in the wrong causal direction.

For our approach, we address the causal inference problem by exploiting an asymmetry in the mean-squared error (MSE) of predicting the cause from the effect and the effect from the cause, respectively, and show, that under appropriate assumptions and in the regime of almost deterministic relations, the prediction error is smaller in causal direction. A preliminary version of this idea can be found in [20, 21] but in these works the analysis is based on a simple heuristic assuming that the regression of Y on X and the regression of X on Y yield functions that are inverse to each other, which holds approximately in the limit of small noise. Moreover, the analysis is also based on the assumption of an additive noise model in causal direction and on having prior knowledge about the functional relation between X and Y , which makes it impractical for generic causal inference problems.

In this work, we aim to generalize and extend the two aforementioned works in several ways: 1) We explicitly allow a dependency between cause and noise. 2) We give a proper mathematical proof of the theory that justifies the method subject to clear formal assumptions. 3) We perform a more extensive evaluation for the application in causal inference and compare it with various related approaches. The theorem stated in this work might also be of interest for general statistical purposes. A briefer version of this work with less extensive experiments and without detailed proofs can be found in [1].

This paper is structured as follows: In Section 2, we introduce the used notations and assumptions, which are necessary for the main theorem of this work stated in Section 3. An algorithm that utilizes this theorem is proposed in Section 4 and evaluated in various artificial and real-world data sets in Section 5.

2 Preliminaries

In the following, we introduce the preliminary notations and assumptions.

2.1 Notation and problem setting

The goal of this paper is to correctly identify cause and effect variable of given observations X and Y . Throughout this paper, a capital letter denotes a random variable and a lowercase letter denotes values attained by the random variable. Variables X and Y are assumed to be real-valued and to have a joint probability density (with respect to the Lebesgue measure), denoted by $p_{X,Y}$. By slightly abusing terminology, we will not further distinguish between a distribution and its density since the Lebesgue measure as a reference is implicitly understood. The notations p_X , p_Y , and $p_{Y|X}$ are used for the corresponding marginal and conditional densities, respectively. The derivative of a function f is denoted by f' .

2.2 General idea

As mentioned before, the general idea of our approach is to simply compare the MSE of regressing Y on X and the MSE of regressing X on Y . If we denote cause and effect by $C, E \in \{X, Y\}$, respectively, our approach explicitly reads as follows. Let ϕ denote the function that minimizes the expected least squares error when predicting E from C , which implies that ϕ is given by the conditional expectation $\phi(c) = \mathbb{E}[E|c]$. Likewise, let ψ be the minimizer of the least squares error for predicting C from E , that is, $\psi(e) = \mathbb{E}[C|e]$. Then we will postulate assumptions that imply

$$\mathbb{E}[(E - \phi(C))^2] \leq \mathbb{E}[(C - \psi(E))^2], \quad (1)$$

in the regime of almost deterministic relations. This conclusion certainly relies on some kind of scaling convention. For our theoretical results we will assume that both X and Y attain values between 0 and 1. However, in some applications, we will also scale X and Y to unit variance to deal with unbounded variables. (1) can be rewritten in terms of conditional variance as

$$\mathbb{E}[\text{Var}[E|C]] \leq \mathbb{E}[\text{Var}[C|E]].$$

2.3 Assumptions

First, recall that we assume throughout the paper that either X is the cause of Y or vice versa in an unconfounded sense, i.e. there is no common cause. To study the limit of an almost deterministic relation in a mathematically precise way, we consider a family of effect variables E_α by

$$E_\alpha := \phi(C) + \alpha N, \quad (2)$$

where $\alpha \in \mathbb{R}^+$ is a parameter controlling the noise level and N is a noise variable that has some (upper bounded) joint density $p_{N,C}$ with C . Note that N here does not need to be statistically independent of C (in contrast to ANMs). Here, ϕ is a function that is further specified below. Therefore, (2) does not, a priori, restrict the set of possible causal relations, because for any pair (C, E) one can define the noise N as the residual $N := E - \phi(C)$ and thus obtain $E_1 = E$ for any arbitrary function ϕ .

For this work, we make use of the following assumptions:

1. **Invertible function:** ϕ is a strictly monotonically increasing two times differentiable function $\phi : [0, 1] \rightarrow [0, 1]$. For simplicity, we assume that ϕ is monotonically increasing with $\phi(0) = 0$ and $\phi(1) = 1$ (similar results for monotonically decreasing functions follow by reflection $E \rightarrow 1 - E$). We also assume that ϕ^{-1} is bounded.
2. **Compact supports:** The distribution of C has compact support. Without loss of generality, we assume that 0 and 1 are the smallest and the largest values, respectively, attained by C . We further assume that the distribution of N has compact support and that there exist values $n_+ > 0 > n_-$ such that for each c , $[n_-, n_+]$ is the smallest interval containing the support of $p_{N|c}$. This ensures that we know $[\alpha n_-, 1 + \alpha n_+]$ is the smallest interval containing the support of p_{E_α} . Then the shifted and rescaled variable

$$\tilde{E}_\alpha := \frac{1}{1 + \alpha n_+ - \alpha n_-} (E_\alpha - \alpha n_-) \quad (3)$$

attains 0 and 1 as minimum and maximum values and thus is equally scaled as C .

3. **Unbiased noise:** We use the convention $\mathbb{E}[N|c] = 0$ for all values c of C without loss of generality (this can easily be achieved by modifying ϕ). Then ϕ is just the conditional expectation, that is, $\phi(c) = \mathbb{E}[E|c]$.

4. **Unit noise variance:** The expected conditional noise variance is $\mathbb{E}[\text{Var}[N|C]] = 1$, which is also not a proper restriction, because we can scale α accordingly since we are only interested in the limit $\alpha \rightarrow 0$.
5. **Independence postulate:** While the above assumptions are just technical, we now state the essential assumption that generates the asymmetry between cause and effect. To this end, we consider the unit interval $[0, 1]$ as probability space with uniform distribution as probability measure. The functions $c \mapsto \phi'(c)$ and $c \mapsto \text{Var}[N|c]p_C(c)$ define random variables on this space, which we postulate to be uncorrelated, formally stated as

$$\text{Cov}[\phi', \text{Var}[N|c]p_C] = 0. \quad (4)$$

More explicitly, (4) reads:

$$\int_0^1 \phi'(c) \text{Var}[N|c]p_C(c)dc - \int_0^1 \phi'(c)dc \int_0^1 \text{Var}[N|c]p_C(c)dc = 0. \quad (5)$$

The justification of (4) is not obvious at all. For the special case where the conditional variance $\text{Var}[N|c]$ is a constant in c (e.g. for ANMs), (4) reduces to

$$\text{Cov}[\phi', p_C] = 0, \quad (6)$$

which is an independence condition for deterministic relations stated in [19]. Conditions of similar type as (6) have been discussed and justified in [14]. They are based on the idea that ϕ contains no information about p_C . This, in turn, relies on the idea that the conditional $p_{E|C}$ contains no information about p_C .

To discuss the justification of (5), observe first that it *cannot* be justified as stating some kind of ‘independence’ between p_C and $p_{E|C}$. To see this, note first that (5) states an uncorrelatedness of the two functions $c \mapsto \phi'(c)$ and $c \mapsto \text{Var}[N|c]p_C(c)$. Since the latter function contains the map $c \mapsto \text{Var}[N|c]$, which is a property of the conditional $p_{E|C}$ and not of the marginal p_C , it thus contains components from both p_C and $p_{E|C}$. Nevertheless, to justify (5) we assume that the function ϕ represents a law of nature that persists when p_C and N change due to changing background conditions. From this perspective, it becomes unlikely that they are related to the background condition at hand. This idea follows the general spirit of ‘modularity and autonomy’ in structural equation modelling, that some structural equations may remain unchanged when other parts of a system change (see Chapter 2 in [4] for a literature review).¹

¹Note, however, that the assignment $E = \phi(C) + N$ is not a structural equation in a strict sense, because then C and N would need to be statistically independent.

A simple implication of (5) reads

$$\int_0^1 \phi'(c) \text{Var}[N|c] p_C(c) dc = 1, \quad (7)$$

due to $\int_0^1 \phi'(c) dc = 1$ and $\int_0^1 \text{Var}[N|c] p_C(c) dc = \text{Var}[N|C] = 1$.

In the following, the term *independence postulate* is referred to the aforementioned postulate and the term *independence* to a statistical independence, which should generally become clear from the context.

3 Theory

As introduced in Section 2.2, we aim to exploit an inequality of the expected prediction errors in terms of $\mathbb{E}[\text{Var}[E|C]] \leq \mathbb{E}[\text{Var}[C|E]]$ to infer the causal direction. Under the aforementioned assumptions, this can be stated if the noise variance is sufficiently small. In order to conclude this inequality and, thus, to justify an application to causal inference, we must restrict our analysis to the case where the noise variance is sufficiently small, since a more general statement is not possible under the aforementioned assumptions. The analysis can be formalized by the ratio of the expectations of the conditional variances in the limit $\alpha \rightarrow 0$.

We will then show

$$\lim_{\alpha \rightarrow 0} \frac{\mathbb{E}[\text{Var}[C|\tilde{E}_\alpha]]}{\mathbb{E}[\text{Var}[\tilde{E}_\alpha|C]]} \geq 1.$$

3.1 Error asymmetry theorem

For our main theorem, we first need an important lemma:

Lemma 1 (Limit of variance ratio) *Let the assumptions 1-4 in Section 2.3 hold. Then the following limit holds:*

$$\lim_{\alpha \rightarrow 0} \frac{\mathbb{E}[\text{Var}[C|\tilde{E}_\alpha]]}{\mathbb{E}[\text{Var}[\tilde{E}_\alpha|C]]} = \int_0^1 \frac{1}{\phi'(c)^2} \text{Var}[N|c] p_C(c) dc \quad (8)$$

The formal proof is a bit technical and is provided in Appendix A, but the idea is quite simple: just think of the scatter plot of an almost deterministic relation as a thick line. Then $\text{Var}[E_\alpha|c]$ and $\text{Var}[C|E_\alpha = \phi(c)]$ are roughly the squared widths of the line at some point $(c, \phi(c))$ measured in vertical and horizontal direction, respectively. The quotient of the widths in vertical and horizontal direction is then

given by the slope. This intuition yields the following approximate identity for small α :

$$\text{Var}[C|\tilde{E}_\alpha = \phi(c)] \approx \frac{1}{(\phi'(c))^2} \text{Var}[\tilde{E}_\alpha|C=c] = \alpha^2 \frac{1}{(\phi'(c))^2} \text{Var}[N|c]. \quad (9)$$

Taking the expectation of (9) over C and recalling that Assumption 4 implies $\mathbb{E}[\text{Var}[\tilde{E}_\alpha|C]] = \alpha^2 \mathbb{E}[\text{Var}[N|C]] = \alpha^2$ already yields (8).

With the help of Lemma 1, we can now formulate the core theorem of this paper, which is shown in Appendix B:

Theorem 1 (Error Asymmetry) *Let the assumptions 1-5 in Section 2.3 hold. Then the following limit always holds*

$$\lim_{\alpha \rightarrow 0} \frac{\mathbb{E}[\text{Var}[C|\tilde{E}_\alpha]]}{\mathbb{E}[\text{Var}[\tilde{E}_\alpha|C]]} \geq 1,$$

with equality only if the functional relation in Assumption 3 is linear.

Note that if ϕ is non-invertible, there is an information loss in anticausal direction, since multiple possible values can be assigned to the same input. Therefore, we can expect that the error difference becomes even higher in these cases, which is supported by the experiments in Section 5.2.2.

3.2 Remark

Theorem 1 states that the inequality holds for all values of α smaller than a certain finite threshold. Whether this threshold is small or whether the asymmetry with respect to regression errors already occurs for large noise cannot be concluded from the above theoretical insights. Presumably, this depends on features of ϕ , p_C , $p_{N|C}$ in a complicated way. However, the experiments in Section 5 suggest that the asymmetry often appears even for realistic noise levels.

4 Algorithm

A causal inference algorithm that exploits Theorem 1 can be formulated in a straightforward way. Given observations X, Y sampled from a joint distribution $p_{X,Y}$, the key idea is to fit regression models in both possible directions and compare the MSE. We call this approach Regression Error based Causal Inference (RECI) and summarize the algorithm in Algorithm 1.

Algorithm 1 The proposed causal inference algorithm.

```
function RECI( $X, Y$ ) ▷  $X$  and  $Y$  are the observed data.
     $(X, Y) \leftarrow \text{RescaleData}(X, Y)$ 
     $f \leftarrow \text{FitModel}(X, Y)$  ▷ Fit regression model  $f: X \rightarrow Y$ 
     $g \leftarrow \text{FitModel}(Y, X)$  ▷ Fit regression model  $g: Y \rightarrow X$ 
     $\text{MSE}_{Y|X} \leftarrow \text{MeanSquaredError}(f, X, Y)$ 
     $\text{MSE}_{X|Y} \leftarrow \text{MeanSquaredError}(g, Y, X)$ 
    if  $\text{MSE}_{Y|X} < \text{MSE}_{X|Y}$  then
        return  $X$  is the cause and  $Y$  is the effect.
    else if  $\text{MSE}_{X|Y} < \text{MSE}_{Y|X}$  then
        return  $Y$  is the cause and  $X$  is the effect.
    else
        return No decision
    end if
end function
```

Although estimating the conditional expectations $\mathbb{E}[Y|X]$ and $\mathbb{E}[X|Y]$ by regression is a standard task in machine learning, we should emphasize that the usual issues of over- and underfitting are critical for our purpose (like for methods based on ANMs or PNLs) because they under- or overestimate the noise levels. It may, however, happen that the method even benefits from underfitting: if there is a simple regression model in causal direction that fits the data quite well, but in anticausal relation the conditional expectation becomes more complex, a regression model with underfitting increases the error even more for the anticausal direction than for the causal direction. This speculative remark is somehow supported by our experiments, where we observed that simple models performed better than complex models, even though they probably did not represent the true conditional expectation.

Also, an accurate estimation of the MSE with respect to the regression model and appropriate preprocessing of the data like removing isolated points in low-density regions, might improve the performance.

5 Experiments

For the experiments, we compared our algorithm with three different related causal inference methods in various artificial and real-world data sets. In each evaluation,

observations of two variables were given and the goal was to correctly identify cause and effect variables.

5.1 Causal inference methods for comparison

In the following, we briefly discuss and compare the causal inference methods which we used for the evaluations.

LiNGAM The model assumptions of LiNGAM are

$$E = \beta C + N,$$

where $\beta \in \mathbb{R}$, $C \perp\!\!\!\perp N$ and N is non-Gaussian. While in real-world data we may often have non-Gaussian noise, the functional relationships are mostly nonlinear. The computational cost is relatively low.

For the experiments, we used a state-of-the-art implementation of LiNGAM that utilizes an entropy based method for calculating the likelihood ratios of the possible causal directions [22]. For this, Eq. (3) in [22] is used in order to estimate the likelihood ratio Eq. (2) in [22].

ANM The ANM approach assumes that

$$E = f(C) + N,$$

where f is nonlinear and $C \perp\!\!\!\perp N$. This method requires fitting a regression function and performing an additional evaluation of the relation between input and residual, which lead to a high computational cost. Important to note is that the choice of the evaluation method is crucial for the performance.

We used an implementation provided by [16], which uses a Gaussian process regression for the prediction and provides different methods for the evaluation of the causal direction. For the experiments, we chose different evaluation methods; *HSIC* for statistical independence tests, an entropy estimator for estimating the mutual information between input and residuals (denoted as *ENT*) and a Bayesian model comparison that assumes Gaussianity (denoted as *FN*). Implementation details and parameters can be found in Table 2 of [16].

IGCI The IGCI approach is able to determine the causal relationship in a deterministic setting

$$E = f(C),$$

under the ‘independence assumption’ $\text{Cov}[\log f', p_C] = 0$. The corresponding algorithm has been applied to noisy causal relations with partial success (and some heuristic justifications [14]), but generalizations of IGCI for non-deterministic relations are actually not known and we consider Assumption 5 in Section 2.3 as first step towards a possibly more general formulation. The computational cost depends on the utilized method for estimating the information criterion, but is generally low. Therefore, IGCI is the fastest of the methods.

For the experiments, we also used an implementation provided by [16], where we always tested all possible combinations of reference measures and information estimators. These combinations are denoted as IGCI_{ij} , where the subscripts indicate:

- $i = \text{U}$: Uniform reference measure (normalizing X and Y)
- $i = \text{G}$: Gaussian reference measure (standardizing X and Y)
- $j = 1$: Entropy estimator using Eq. (12) in [13]
- $j = 2$: Integral approximation of Eq. (13) in [13]
- $j = 3$: Integral approximation of Eq. (22) in [16]

CURE CURE is based on the idea that the distribution p_C does not help in better regressing E on C , while the distribution p_E may help in better regressing C on E . CURE implements this idea in a Bayesian way via a modified Gaussian process regression. However, since CURE requires the generation of Markov-Chain-Monte-Carlo (MCMC) samples, the biggest drawback is a very high computational cost.

An implementation of CURE by the authors has been provided for our experiments. Here, we used similar settings as described in Section 6.2 of [15], where 200 data samples were used and 10000 MCMC samples were generated. The number of internal repetitions depends on the experimental setting.

RECI Our approach addresses non-deterministic nonlinear relations and, in particular, allows a dependency between cause and noise. Since we only require the fitting of a least-squares solution in both possible causal directions, RECI can be easily implemented, does not rely on any independence tests and, depending on the regression model and implementation details, can be performed quickly.

In the experiments, we have always used the same class of regression function for the causal and anticausal direction to compare the errors, but performed multiple experiments with different function classes. For each evaluation, we randomly split the data into training and test data, where we tried different ratios. The utilized regression models were:

- a logistic function (LOG) of the form $a + (b - a)/(1 + \exp(c \cdot (d - x)))$
- shifted monomial functions (MON) of the form $ax^n + b$ with $n \in [2, 9]$
- polynomial functions (POLY) of the form $\sum_{i=0}^k a_i x^i$ with $k \in [1, 9]$
- support vector regression (SVR) with a linear kernel
- neural networks (NN) with different numbers of hidden neurons: 2, 5, 10, 20, 2-4, 4-8, where '-' indicates two hidden layers

The logistic and monomial functions cover rather simple regression models, which are probably not able to capture the true function f in most cases. On the other hand, support vector regression and neural networks should be complex enough to capture f . The polynomial functions are rather simple too, but more flexible than the logistic and monomial functions.

We used the standard Matlab implementation of these methods and have always chosen the default parameters, where the parameters of LOG, MON and POLY were fitted by minimizing the least-squared error.

During the experiments, we observed that the MSE varied a lot in many data sets due to relatively small sample sizes and the random selection of training and test data. Therefore, we averaged the MSE over all performed runs first before comparing them, seeing that this should give more accurate estimations of $\mathbb{E}[\text{Var}[Y|X]]$ and $\mathbb{E}[\text{Var}[X|Y]]$ with respect to the class of the regression function. Since the performances of averaging the MSE over multiple runs were better than only a single run and since we did not optimize the choice of regression functions for each setting, we only summarize the results of the best performing MON, POLY and NN setups of each setting in the following. A detailed overview of all results, including the performance of estimating the MSE in single runs, can be found in Appendix D.

General Remark Each evaluation was performed in the original data sets and in preprocessed versions where isolated points (low-density points) were removed. For the latter, we used the implementation and parameters from [15], where a kernel density estimator with a Gaussian kernel is utilized. Note that CURE per default uses this preprocessing step, also in the original data. In all evaluations, we forced a decision by the algorithms, where in case of ANM the direction with the highest score of the independence test was taken.

Except for CURE, we averaged the performances of each method over 100 runs, where we uniformly sampled 500 data points for ANM and SVR if the data set contains more than 500 data points. For CURE, we only performed four internal repetitions in the artificial and eight internal repetitions in the real-world data sets due to the high computational cost. Since we used all data points for IGCI and LiNGAM, these methods have a consistent performance over all runs.

5.2 Artificial data

For experiments with artificial data, we performed evaluations with simulated cause-effect pairs generated for a benchmark comparison in [16]. Further, we generated additional pairs with linear, nonlinear invertible and nonlinear non-invertible functions where input and noise are strongly dependent.

5.2.1 Simulated benchmark cause-effect pairs

The work of [16] provides simulated cause-effect pairs with randomly generated distributions and functional relationships under different conditions. As pointed out by [16], the scatter plots of these simulated data look similar to those of real-world data. We took the same data sets as used in [16] and extended the reported results with an evaluation with CURE, LiNGAM, RECI and further provide results in the preprocessed data.

The data sets are categorized into four different categories:

- SIM: Pairs without confounders. The results are shown in Figure 1(a)-1(b)
- SIM-c: A similar scenario as SIM, but with one additional confounder. The results are shown in Figure 1(c)-1(d)
- SIM-1n: Pairs with low noise level without confounder. The results are shown in Figure 2(a)-2(b)

- SIM-G: Pairs where the distributions of C and N are almost Gaussian without confounder. The results are shown in Figure 2(c)-2(d)

The general form of the data generation process without confounder but with measurement noise² is

$$\begin{aligned} C' &\sim p_C, N \sim p_N \\ N_C &\sim \mathcal{N}(0, \sigma_C), N_E \sim \mathcal{N}(0, \sigma_E) \\ C &= C' + N_C \\ E &= f_E(C', N) + N_E \end{aligned}$$

and with confounder

$$\begin{aligned} C' &\sim p_C, N \sim p_N, Z \sim p_Z \\ C'' &= f_C(C', Z) \\ N_C &\sim \mathcal{N}(0, \sigma_C), N_E \sim \mathcal{N}(0, \sigma_E) \\ C &= C'' + N_C \\ E &= f_E(C'', Z, N) + N_E, \end{aligned}$$

where N_C, N_E represent independent observational Gaussian noise and the variances σ_C and σ_E are chosen randomly with respect to the setting.³ More details can be found in Appendix C of [16].

Generally, ANM performs the best in all data sets. However, the difference between ANM and RECI, depending on the regression model, becomes smaller in the preprocessed data where isolated points were removed. According to the observed performances, removing these points seems to often improve the accuracy of RECI, but decrease the accuracy of ANM.

In all data sets, except for SIM-G, RECI always outperforms IGCI, CURE and LiNGAM if a simple logistic or polynomial function is utilized for the regression. However, in the SIM-G data set, our approach performs comparably poor, which could be explained by the violation of the assumption of a compact support. In this nearly Gaussian data, IGCI performs the best with a Gaussian reference measure.

²Note, however, that adding noise to the cause (as it is done here) can also be considered as a kind of confounding. Actually, C' is the cause of E in the below generating model, while the noisy version C is not the cause of E . Accordingly, C' is the hidden common cause of C and E . Here we refer to the scenario as an unconfounded case with measurement noise as in [16].

³Note that only N_E is Gaussian, while the regression residual is non-Gaussian due to the non-linearity of f_E and non-Gaussianity of N, Z .

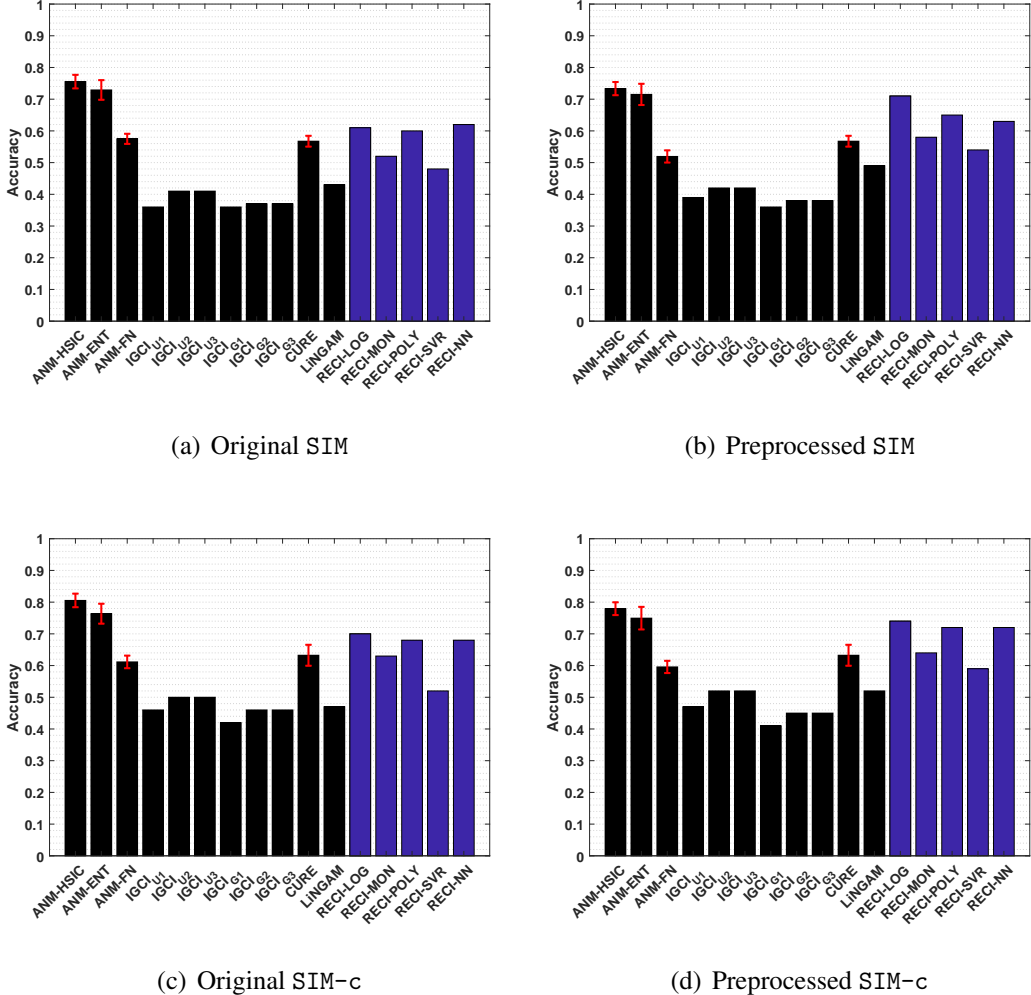


Figure 1: Evaluation result of all methods in the SIM and SIM-c data sets. The figures on the left side show the results of the evaluations in the original data and on the right side the results in the preprocessed versions where low-density points were removed.

However, we also evaluated RECI with standardized data in the SIM-G data sets, which is equivalent to a Gaussian reference measure for IGCI. A summary of the results can be found in Figures 7(c)-7(d) in Appendix C and more detailed results in Table 4 and Table 5 in Appendix D. These results are significantly better than

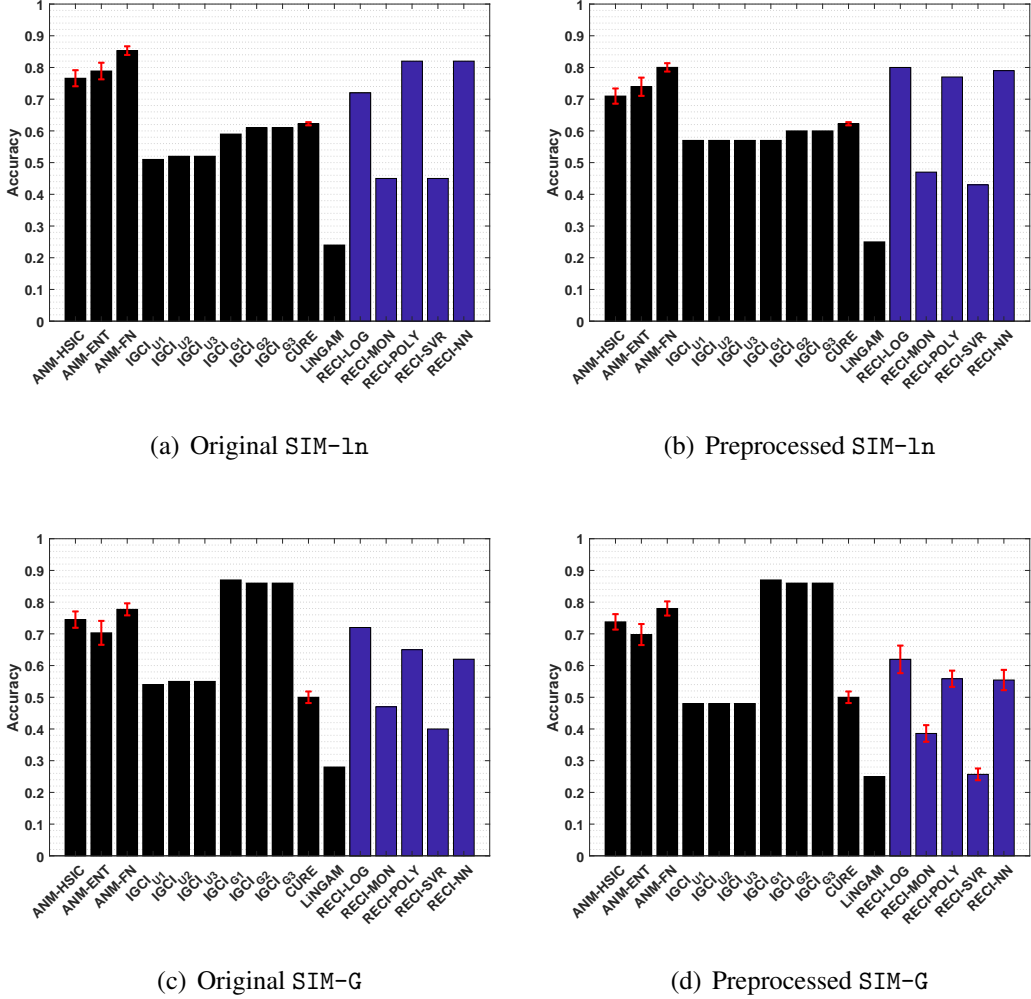


Figure 2: Evaluation result of all methods in the SIM-1n and SIM-G data sets. The figures on the left side show the result of the evaluations in the original data and on the right side the results in the preprocessed versions where low-density points were removed.

normalizing the data in this case. However, although our theorem only justifies a normalization, a different scaling, such as standardization, might be a reasonable alternative.

Even though Theorem 1 does not exclude cases of a high noise level, it makes

a clear statement about low level noise. Therefore, as expected, RECI performs the best in SIM-1n, where the noise level is low. In all cases, LiNGAM performs very poorly due to the violations of its core assumptions.

ANM and RECI require a least-squares regression, but ANM additionally depends on an independence test, which can have a high computational cost and a big influence on the performance. Therefore, even though RECI does not outperform ANM, it represents a competitive alternative with a lower computational cost, depending on the regression model and MSE estimation. Also, seeing that RECI explicitly allows both cases, a dependency and an independency between C and N while ANM only allows the latter, it can be expected that RECI performs significantly better than ANM in cases where the dependency between C and N is strong. This is evaluated in Section 5.2.2. In comparison with IGCI, LiNGAM and CURE, RECI outperforms in almost all data sets. Note that [16] performed more extensive experiments and show more comparisons with ANM and IGCI in these data sets, where additional parameter configurations were tested. However, they report no results for the preprocessed data.

5.2.2 Simulated cause-effect pairs with strong dependent noise

Since the data sets of the evaluations in Section 5.2.1 are generated by structural equations with independence noise variables, we additionally performed evaluations with artificial data sets where the input distribution and the noise distribution are strongly dependent. For this, we considered a similar data generation process as described in [13]. We generated data with various different cause and noise distributions, different functions and varying values for $\alpha \in [0, 1]$. In order to ensure a dependency between C and N , we additionally introduced two unobserved source variables S_1 and S_2 that are randomly sampled from different distributions. Variables C and N then consist of a randomly weighted linear combination of S_1 and S_2 . The general causal structure of these data sets is illustrated in Figure 3. All used distributions for the source variables and all used functions can be found in Table 1, where $GM_{\mu, \sigma}$ denotes a Gaussian mixture distribution with density $PGM_{\mu, \sigma}(c) = \frac{1}{2}(\varphi(c|\mu_1, \sigma_1) + \varphi(c|\mu_2, \sigma_2))$ and Gaussian pdf $\varphi(c|\mu, \sigma)$.

Apart from rather simple functions for ϕ , [13] proposed to generate more general functions in the form of convex combinations of mixtures of cumulative Gaussian distribution functions $\psi(C|\mu_i, \sigma_i)$:

$$s_n(C) = \sum_{i=1}^n \beta_i \psi(C|\mu_i, \sigma_i),$$

Table 1: All distributions p_S , functions ϕ and functions f that were used for the generation of the Linear, Non-invertible and Invertible data sets. In case of the functions for Non-invertible, $\text{rescale}(X, -n, n)$ denotes a rescaling of the input data X on $[-n, n]$.

p_S	Data set	$\phi(C)$
$U(0, 1)$	Linear	C
$\mathcal{N}(0, \sigma^2)$	Invertible	$s_5(C)$
$\mathcal{N}(0.5, \sigma^2)$	Non-invertible	$\text{rescale}(C, -2, 2)^2$
$\mathcal{N}(1, \sigma^2)$		$\text{rescale}(C, -2, 2)^4$
$GM_{[0.3, 0.7]^T, [0.1, 0.1]^T}$		$\sin(\text{rescale}(C, -2 \cdot \pi, 2 \cdot \pi))$
		$\frac{f(X)}{X}$
		$\exp(X)$
		$s_5(X)$

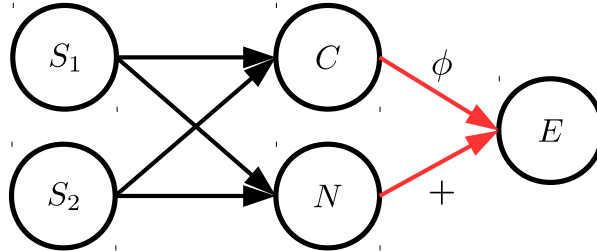


Figure 3: The general structure of the data generation process where C and N are dependent. In order to achieve this, cause and noise consist of a mixture of two sources S_1 and S_2 .

where $\beta_i, \mu_i \in [0, 1]$ and $\sigma_i \in [0, 0.1]$. For the experiments, we set $n = 5$ and chose the parameters of $s_5(C)$ randomly according to the uniform distribution. Note that $\psi(C|\mu_i, \sigma_i)$ is always monotonically increasing and thus $s_5(C)$ can have an arbitrary random shape while being monotonically increasing.

Cause-effect pairs were then generated in the following way:

$$\begin{aligned}
w_1, w_2 &\sim U(0, 1) \\
S_1, S_2 &\sim p_S \\
S_1 &= S_1 - \mathbb{E}[S_1] \\
S_2 &= S_2 - \mathbb{E}[S_2] \\
C' &= w_1 \cdot f_1(S_1) + (1 - w_1) \cdot f_2(S_2) \\
N' &= w_2 \cdot f_3(S_1) + (1 - w_2) \cdot f_4(S_2) \\
C &= \text{normalize}(C') \\
N &= \alpha \cdot \text{normalizeVariance}(N') \\
E &= \phi(C) + N,
\end{aligned}$$

where the distributions of S_1 and S_2 and the functions f_1, f_2, f_3, f_4 were chosen randomly from p_S and f in Table 1, respectively. Note that S_1 and S_2 can follow different distributions. The choice of ϕ depends on the data set, where we differentiated between three data sets:

- **Linear:** Only the identity function $\phi(C) = C$
- **Invertible:** Arbitrary invertible functions $\phi(C) = s_5(C)$
- **Non-invertible:** Functions that are not invertible on the respective domain

In total, we generated 100 data sets for each value of parameter α , which controls the amount of noise in the data. In each generated data set, we randomly chose different distributions and functions. For Linear and Invertible the step size of α is 0.1 and for Non-invertible 0.025. Here, we only performed one repetition on each data set for all algorithms. Figure 4(a)-4(c) summarize all results and Table 7 in Appendix D shows the best performing functions and parameters of the different causal inference methods. Note that we omitted experiments with CURE in these data sets due to the high computational cost.

Linear: As expected, ANM, IGCI and RECI perform very poorly, since they require nonlinear data. In case of RECI, Theorem 1 states an equality of the MSE if the functional relation is linear and, thus, the causal direction can not be inferred. While LiNGAM performs well for $\alpha = 0.1$, and probably for smaller values of α too, the performance drops if α increases. The poor performances of

LiNGAM and ANM can also be explained by the violation of its core assumption of an independence between cause and input.

Invertible: In this data set, IGCI performs quite well for small α , since all assumptions approximately hold, but the performance decreases when the noise becomes stronger and violates the assumption of a deterministic relation. In case of RECI, we made a similar observation, but it performs much better than IGCI if $\alpha < 0.5$. Aside from the assumption of linear data for LiNGAM, the expected poor performance of LiNGAM and ANM can be explained by the violation of the independence assumption between C and N .

Non-invertible: These results seem very interesting, since it supports the argument that the error asymmetry becomes even more clearer if the function is not invertible due to an information loss of regressing in anticausal direction. On the other hand, IGCI performs reasonably well, while ANM and LiNGAM perform even worse than a baseline of just guessing. The constant results of each method can be explained by the rather simple and similar choice of data generating functions.

While the cause and noise also have a dependency in the SIM-c data sets, the performance gap between ANM and RECI is vastly greater in Invertible and Non-invertible than in SIM-c due to a strong violation of the independent noise assumption. Therefore, RECI might perform better than ANM in cases with a strong dependency between cause and noise.

5.3 Real-world data

In real-world data, the true causal relationship generally requires expert knowledge and can still lead to rather philosophical discussions in unclear cases. For our evaluations, we considered the commonly used cause-effect pairs (CEP) benchmark data sets. These benchmark data sets provided, at the time of these evaluations, 106 data sets with given cause and effect variables.⁴ However, since we only consider a two variable problem, we omit the multivariate data sets, which leaves 100 data sets for the evaluations. Each data set comes with a corresponding weight. This is because several data sets are too similar to consider them as independent examples, hence they get lower weights. Therefore, the accuracy is

⁴The data set can be found on <https://webdav.tuebingen.mpg.de/cause-effect/>. More details and discussion about the causal relationship of the first 100 pairs can be found in [16].

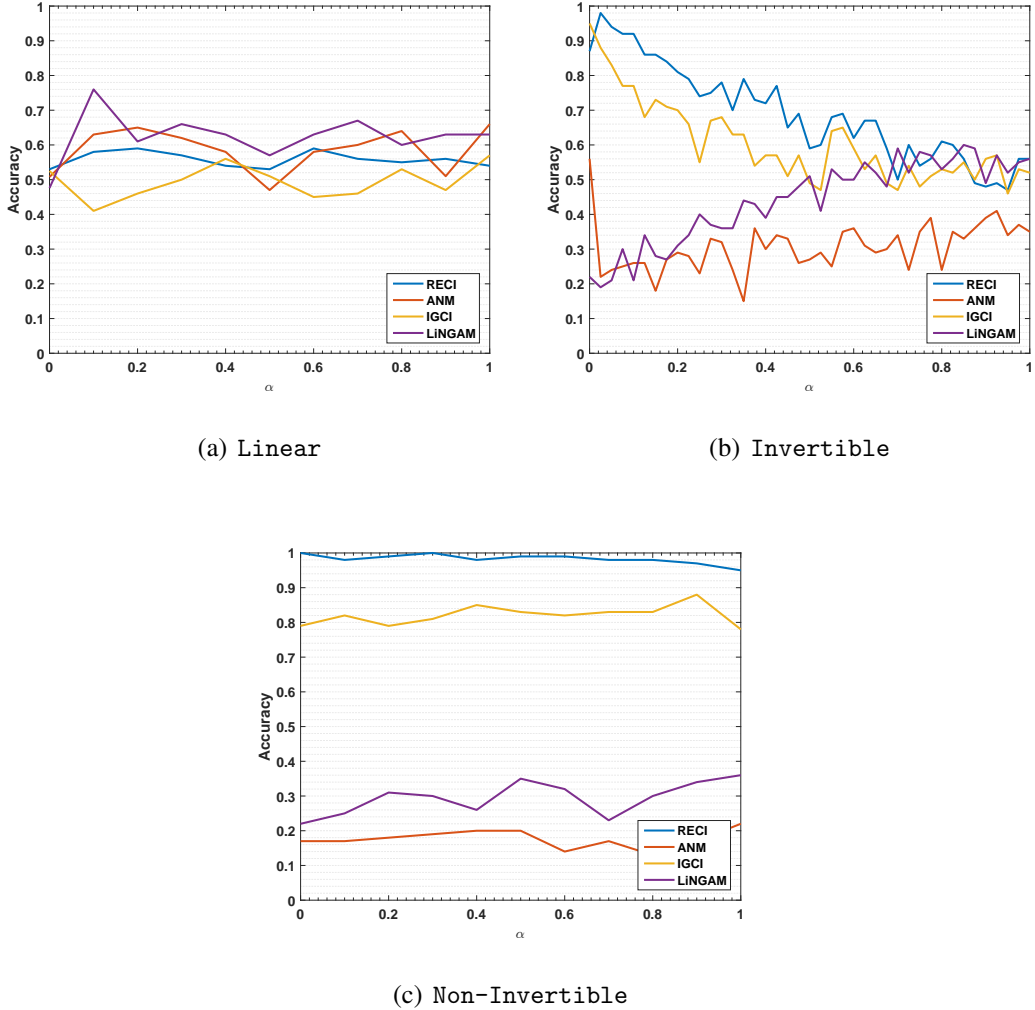


Figure 4: Evaluation result of all methods in the Linear, Invertible and Non-Invertible data sets. The parameter α controls the amount of noise in the data.

calculated in the following way

$$\text{accuracy} = \frac{\sum_{m=1}^M w_m \delta_{\hat{d}_m, d_m}}{\sum_{m=1}^M w_m},$$

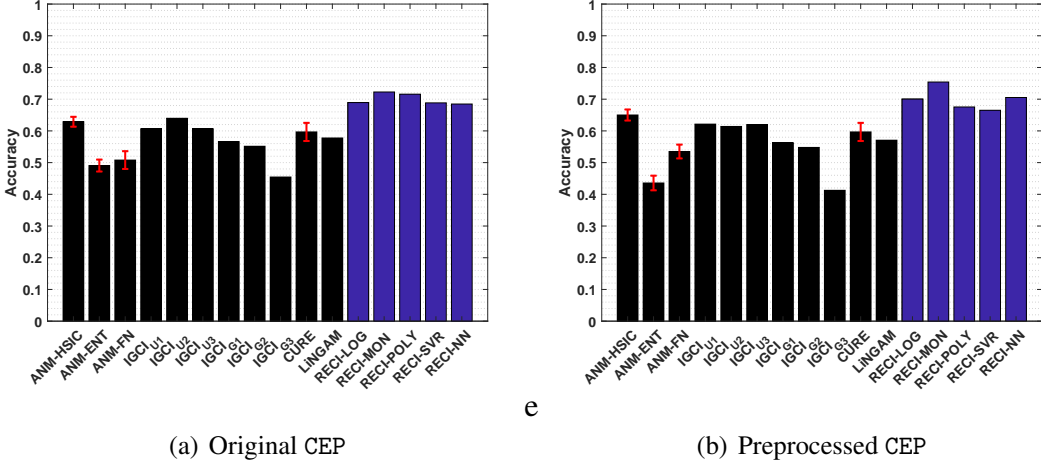


Figure 5: Evaluation result of all methods in the real-world CEP data sets. The figure on the left side shows the result of the evaluations in the original data and on the right side the results in the preprocessed versions where low-density points were removed.

where M is the number of data sets, w_m the weight of data set m , d_m the correct causal direction and \hat{d}_m the inferred causal direction of the corresponding method. The experimental setup is the same as for the artificial data sets, but we doubled the number of internal repetition of CURE to eight times in order to provide the same experimental conditions as in [15].

Figure 5(a) and 5(b) shows the results of the evaluations in the original and preprocessed data, respectively. In all cases, RECI performs better than all other methods.⁵ Further, the performance difference gap even increases in the preprocessed data with removed low-density points. Surprisingly, as Table 2 in Appendix D indicates, the very simple monomial functions $ax^3 + c$ and $ax^2 + c$ perform the best, even though it is very unlikely that these functions are able to capture the true function ϕ . We obtained similar observations in the artificial data sets.

In order to show that RECI still performs reasonably well under a different scaling, we also evaluated RECI in the real-world data set with standardized data.

⁵The work of [16] provides further evaluations of ANM and IGCI in the original CEP data set with parameter configurations that reached slightly higher accuracies than the presented results in this work. Regarding CURE, we had to use a simplified implementation due to the high computational cost, which did not perform as well as the results reported in [15].

Algorithm 2 Causal inference algorithm that uses (10) as rejection criterion.

```
function RECI( $X, Y, t$ )       $\triangleright X$  and  $Y$  are the observed data and  $t \in [0, 1]$  the  
threshold for rejecting a decision.  
   $(X, Y) \leftarrow \text{RescaleData}(X, Y)$   
   $f \leftarrow \text{FitModel}(X, Y)$                        $\triangleright$  Fit regression model  $f: X \rightarrow Y$   
   $g \leftarrow \text{FitModel}(Y, X)$                        $\triangleright$  Fit regression model  $g: Y \rightarrow X$   
   $\text{MSE}_{Y|X} \leftarrow \text{MeanSquaredError}(f, X, Y)$   
   $\text{MSE}_{X|Y} \leftarrow \text{MeanSquaredError}(g, Y, X)$   
   $\xi \leftarrow \frac{\min(\text{MSE}_{X|Y}, \text{MSE}_{Y|X})}{\max(\text{MSE}_{X|Y}, \text{MSE}_{Y|X})}$   
  if  $\xi \leq t$  and  $\text{MSE}_{Y|X} \neq \text{MSE}_{X|Y}$  then  
    if  $\text{MSE}_{Y|X} < \text{MSE}_{X|Y}$  then  
      return  $X$  is the cause and  $Y$  is the effect.  
    else  
      return  $Y$  is the cause and  $X$  is the effect.  
    end if  
  else  
    return No decision  
  end if  
end function
```

These results can be found summarized in Figures 7(a)-7(b) in Appendix C and more detailed in Table 4 and Table 5 in Appendix D. While standardizing the data improve the performance in the SIM-G data, it slightly decreases the performance in the real-world data as compared to a normalization of the data, but still performs reasonably well. This shows some robustness with respect to a different scaling.

5.4 Error ratio as rejection criterion

It is not clear how to define a confidence measure for the decision of RECI. However, since Theorem 1 states that the correct causal direction has a smaller error, we evaluated the idea of using the error ratio

$$\frac{\min(\mathbb{E}[\text{Var}[X|Y]], \mathbb{E}[\text{Var}[Y|X]])}{\max(\mathbb{E}[\text{Var}[X|Y]], \mathbb{E}[\text{Var}[Y|X]])} \quad (10)$$

as a rejection criterion for a decision. The idea is that the smaller the error ratio the higher the confidence of the decision due to the large error difference. Note

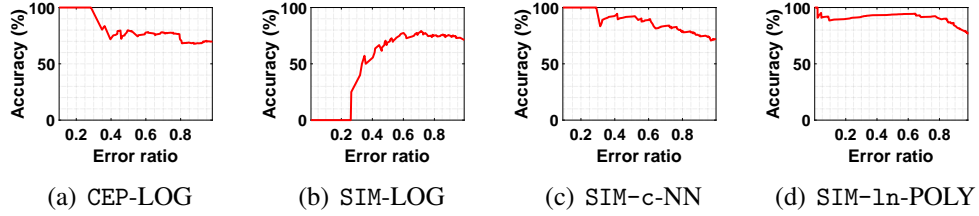


Figure 6: The exemplary performance of RECI with respect to the error ratio (10) as rejection criterion. A small ratio indicates a high error difference.

that we formulated the ratio inverse to Theorem 1 in order to get a value on $[0, 1]$. Algorithm 1 can be modified in a straight forward manner to utilize this error ratio. The modification is summarized in Algorithm 2.⁶

We re-evaluated the experimental results by considering only data sets where Algorithm 2 returns a decision. Figures 6(a)-6(d) show some examples of the performance of RECI if we use the error ratio as rejection criterion. In the figures, an error ratio of 0.2, for instance, can be seen as a surrogate indicator of RECI's accuracy if we only consider data sets where the error ratio was ≤ 0.2 and exclude data sets where the error ratio was > 0.2 . In this sense, we can get an idea of how useful the error ratio is as rejection criterion. While Figures 6(a), 6(c) and 6(d) support the intuition that the smaller the error ratio, the higher the decision confidence, Figure 6(b) has a contradictive behavior. Generally, it seems that a small error ratio (big error difference) is rather an indicator for an uncertain decision, while an error ratio > 0.3 might be a more reliable indicator. Note that in the most cases, depending on the regression model and scenario, the majority of data sets have an error ratio between 0.3 and 0.9. All plots for the original data can be found in Figure 8, all plots for the preprocessed data in Figure 9 and all plots for the standardized data in Figure 10 in Appendix E.

5.5 Discussion

Due to the greatly varying behavior and the choice of various optimization parameters, a clear rule of which regression function is the best choice for RECI remains an unclear and difficult problem. Overall, it seems that simple functions are better in capturing the error asymmetries than complex models. However, a

⁶Algorithm 1 and Algorithm 2 are equivalent if $t = 1$.

clear explanation for this is still lacking. A possible reason for this might be that simple functions in causal direction already achieve a small error, while in anticausal direction, more complex models are required to achieve a small error.⁷ Regarding the removal of low-density points, the performance of methods that are based on the Gaussianity assumption, such as FN and IGCI with Gaussian reference measure, seems not to be influenced by the removal. On the other hand, the performance of HSIC, ENT, and IGCI with uniform measure is negatively affected, while the performance of LiNGAM and RECI increases. In case of RECI, this can be explained by a better estimation of the true MSE with respect to the regression function class.

Regarding the computational cost, we want to emphasize again that RECI, depending on the implementation details, can have a significantly lower computational cost than ANM and CURE, while providing comparable or even better results. Further, it can be easily implemented and applied.

6 Conclusion

We presented an approach for causal inference based on an asymmetry in the prediction error. Under the assumption of an independence among the data generating function, the noise, and the distribution of the cause, we proved (in the limit of small noise) that the conditional variance of predicting the cause by the effect is greater than the conditional variance of predicting the effect by the cause. Here, the additive noise is not assumed to be independent of the cause (in contrast to so-called additive noise models). The stated theorem might also be interesting for other statistical applications.

We proposed an easily implementable and applicable algorithm, which we call RECI, that exploits this asymmetry for causal inference. The evaluations show supporting results and leave room for further improvements. By construction, the performance of RECI depends on the regression method. According to our limited

⁷To justify speculative remarks of this kind raises deep questions about the foundations of causal inference. Using algorithmic information theory, one can, for instance, show that the algorithmic independence of p_C and $p_{E|C}$ implies

$$K(p_C) + K(p_{E|C}) \leq K(p_E) + K(p_{C|E}),$$

if K denotes the description length of a distribution in the sense of Kolmogorov complexity, for details see Section 4.1.9 in [4]. In this sense, appropriate independence assumptions between p_C and $p_{E|C}$ imply that $p_{E,C}$ has a simpler description in causal direction than in anticausal direction.

experience so far, regression with simple model classes (that tend to underfit the data) performs reasonably well. To clarify whether this happens because the conditional distributions tend to be simpler – in a certain sense – in causal direction than in anticausal direction has to be left for the future.

Appendices

A Proof of Lemma 1

We first give some reminders of the definition of the conditional variance and some properties. For two random variables Z, Q the conditional variance of Z , given q is defined by

$$\text{Var}[Z|q] := \mathbb{E}[(Z - \mathbb{E}[Z|q])^2|q],$$

while $\text{Var}[Z|Q]$ is the random variable attaining the value $\text{Var}[Z|q]$ when Q attains the value q . Its expectation reads

$$\mathbb{E}[\text{Var}[Z|Q]] := \int \text{Var}[Z|q] p_Q(q) dq.$$

For any $a \in \mathbb{R}$, we have

$$\text{Var}\left[\frac{Z}{a}|q\right] = \frac{\text{Var}[Z|q]}{a^2}.$$

For any function h we have

$$\text{Var}[h(Q) + Z|q] = \text{Var}[Z|q],$$

which implies $\text{Var}[h(Q)|q] = 0$. Moreover, we have

$$\text{Var}[Z|h(q)] = \text{Var}[Z|q],$$

if h is invertible.

To begin the main part of the proof, we first observe

$$\mathbb{E}[\text{Var}[E_\alpha|C]] = \mathbb{E}[\text{Var}[\phi(C) + \alpha N|C]] = \alpha^2 \underbrace{\mathbb{E}[\text{Var}[N|C]]}_{= 1 \text{ (Assumpt. 4)}} = \alpha^2. \quad (11)$$

Moreover, one easily verifies that

$$\lim_{\alpha \rightarrow 0} \frac{\mathbb{E}[\text{Var}[C|\tilde{E}_\alpha]]}{\mathbb{E}[\text{Var}[\tilde{E}_\alpha|C]]} = \lim_{\alpha \rightarrow 0} \frac{\mathbb{E}[\text{Var}[C|E_\alpha]]}{\mathbb{E}[\text{Var}[E_\alpha|C]]}, \quad (12)$$

due to (3) provided that these limits exist. Combining (11) and (12) yields

$$\lim_{\alpha \rightarrow 0} \frac{\mathbb{E}[\text{Var}[C|\tilde{E}_\alpha]]}{\mathbb{E}[\text{Var}[\tilde{E}_\alpha|C]]} = \lim_{\alpha \rightarrow 0} \frac{\mathbb{E}[\text{Var}[C|E_\alpha]]}{\alpha^2} = \lim_{\alpha \rightarrow 0} \mathbb{E} \left[\text{Var} \left[\frac{C}{\alpha} \middle| E \right] \right]. \quad (13)$$

Now, we can rewrite (13) as

$$\begin{aligned} \lim_{\alpha \rightarrow 0} \mathbb{E} \left[\text{Var} \left[\frac{C}{\alpha} \middle| E_\alpha \right] \right] &= \lim_{\alpha \rightarrow 0} \mathbb{E} \left[\text{Var} \left[\frac{\phi^{-1}(E_\alpha - \alpha N)}{\alpha} \middle| E_\alpha \right] \right] \\ &= \lim_{\alpha \rightarrow 0} \int_{\phi(0) + \alpha n_-}^{\phi(1) + \alpha n_+} \text{Var} \left[\frac{\phi^{-1}(e - \alpha N)}{\alpha} \middle| e \right] p_{E_\alpha}(e) de \\ &= \lim_{\alpha \rightarrow 0} \int_{\phi(0)}^{\phi(1)} \text{Var} \left[\frac{\phi^{-1}(e - \alpha N)}{\alpha} \middle| e \right] p_{E_\alpha}(e) de, \end{aligned} \quad (14)$$

where in the latter step we exploit that the function

$$e \mapsto \text{Var} \left[\phi^{-1}(e - \alpha N) / \alpha \middle| e \right] p_{E_\alpha}(e)$$

is uniformly bounded in α . This is because, first, ϕ^{-1} attains only values in $[0, 1]$, and hence the variance is bounded by 1. Second, $p_{E_\alpha}(e)$ is uniformly bounded due to

$$\begin{aligned} p_{E_\alpha}(e) &= \int_{n_-}^{n_+} p_{\phi(C), N}(e - \alpha n, n) dn = \int_{n_-}^{n_+} p_{C, N}(\phi^{-1}(e - \alpha n), n) \phi^{-1}'(e - \alpha n) dn \\ &\leq \|\phi^{-1}'\|_\infty \|p_{C, N}\|_\infty (n_+ - n_-). \end{aligned}$$

Hence, the bounded convergence theorem states

$$\lim_{\alpha \rightarrow 0} \int_{\phi(0)}^{\phi(1)} \text{Var} \left[\frac{\phi^{-1}(e - \alpha N)}{\alpha} \middle| e \right] p_{E_\alpha}(e) de = \int_{\phi(0)}^{\phi(1)} \lim_{\alpha \rightarrow 0} \left(\text{Var} \left[\frac{\phi^{-1}(e - \alpha N)}{\alpha} \middle| e \right] p_{E_\alpha}(e) \right) de.$$

To compute the limit of

$$\text{Var} \left[\frac{\phi^{-1}(e - \alpha N)}{\alpha} \middle| e \right],$$

we use Taylor's theorem to obtain

$$\phi^{-1}(e - \alpha n) = \phi^{-1}(e) - \alpha n \phi^{-1}'(e) - \frac{\alpha^2 n^2 \phi^{-1}''(E_2(n, e))}{2}, \quad (15)$$

where $E_2(n, e)$ is a real number in the interval $(e - \alpha n, e)$. Since (15) holds for every $n \in [-\frac{e}{\alpha}, \frac{1-e}{\alpha}]$ (note that ϕ and ϕ^{-1} are bijections of $[0, 1]$, thus $e + \alpha n$ lies in $[0, 1]$) it also holds for the random variable N if $E_2(n, e)$ is replaced with the random variable $E_2(N, e)$ (here, we have implicitly assumed that the map $n \mapsto e_2(n, e)$ is measurable). Therefore, we see that

$$\begin{aligned} \lim_{\alpha \rightarrow 0} \text{Var} \left[\frac{\phi^{-1}(e - \alpha N)}{\alpha} \middle| e \right] &= \lim_{\alpha \rightarrow 0} \text{Var} \left[-N \phi^{-1}'(e) - \frac{\alpha N^2 \phi^{-1}''(E_2(N, e))}{2} \middle| e \right] \\ &= \phi^{-1}'(e)^2 \text{Var}[N|e]. \end{aligned} \quad (16)$$

Moreover, we have

$$\lim_{\alpha \rightarrow 0} p_{E_\alpha}(e) = p_{E_0}(e). \quad (17)$$

Inserting (17) and (16) into (14) yields

$$\begin{aligned} \lim_{\alpha \rightarrow 0} \mathbb{E} \left[\text{Var} \left[\frac{C}{\alpha} \middle| E_0 \right] \right] &= \int_{\phi(0)}^{\phi(1)} \phi^{-1}'(e)^2 \text{Var}[N|e] p_{E_0}(e) de \\ &= \int_0^1 \phi^{-1}'(\phi(c))^2 \text{Var}[N|\phi(c)] p_C(c) dc \\ &= \int_0^1 \frac{1}{\phi'(c)^2} \text{Var}[N|\phi(c)] p_C(c) dc, \end{aligned}$$

where the second equality is a variable substitution using the deterministic relation $E_0 = \phi(C)$ (which implies $p_{E_0}(\phi(c)) = p_C(c)/\phi'(c)$ or, equivalently, the simple symbolic equation $p_{E_0}(e)de = p_C(c)dc$). This completes the proof due to (13). \square

B Proof of Theorem 1

We first recall that Lemma 1 states

$$\lim_{\alpha \rightarrow 0} \frac{\mathbb{E}[\text{Var}[C|\tilde{E}_\alpha]]}{\mathbb{E}[\text{Var}[\tilde{E}_\alpha|C]]} = \int_0^1 \frac{1}{\phi'(c)^2} \text{Var}[N|c] p_C(c) dc.$$

We then have

$$\begin{aligned}
& \int_0^1 \frac{1}{\phi'(c)^2} \text{Var}[N|c] p_C(c) dc \\
&= \int_0^1 \frac{1}{\phi'(c)^2} \text{Var}[N|c] p_C(c) dc \cdot \underbrace{\int_0^1 \text{Var}[N|c] p_C(c) dc}_{= 1 \text{ (Assumpt. 4)}} \\
&= \int_0^1 \sqrt{\left(\frac{1}{\phi'(c)}\right)^2 \text{Var}[N|c]} p_C(c) dc \cdot \int_0^1 \sqrt{\text{Var}[N|c]}^2 p_C(c) dc \\
&\geq \left(\int_0^1 \sqrt{\left(\frac{1}{\phi'(c)}\right)^2 \text{Var}[N|c]} \sqrt{\text{Var}[N|c]} p_C(c) dc \right)^2 \\
&= \left(\int_0^1 \frac{1}{\phi'(c)} \text{Var}[N|c] p_C(c) dc \right)^2,
\end{aligned} \tag{18}$$

where the inequality is just the Cauchy Schwarz inequality applied to the bilinear form $f, g \mapsto \int f(c)g(c)p_C(c)dc$ for the space of functions f for which $\int f^2(c)p_C(c)dc$ exists. We can make a statement about (18) in a similar way by using (7) implied by the independence postulate and using Cauchy Schwarz:

$$\begin{aligned}
& \int_0^1 \frac{1}{\phi'(c)} \text{Var}[N|c] p_C(c) dc \\
&= \int_0^1 \frac{1}{\phi'(c)} \text{Var}[N|c] p_C(c) dc \cdot \underbrace{\int_0^1 \phi'(c) \text{Var}[N|c] p_C(c) dc}_{= 1 \text{ (7)}} \\
&= \int_0^1 \sqrt{\frac{1}{\phi'(c)} \text{Var}[N|c]} p_C(c) dc \cdot \int_0^1 \sqrt{\phi'(c) \text{Var}[N|c]}^2 p_C(c) dc \\
&\geq \left(\int_0^1 \sqrt{\frac{1}{\phi'(c)} \text{Var}[N|c]} \sqrt{\phi'(c) \text{Var}[N|c]} p_C(c) dc \right)^2 \\
&= \left(\underbrace{\int_0^1 \text{Var}[N|c] p_C(c) dc}_{= 1 \text{ (Assumpt. 4)}} \right)^2 = 1.
\end{aligned} \tag{19}$$

Combining (18) and (19) with Lemma 1 completes the proof.

□

C Results of standardized data

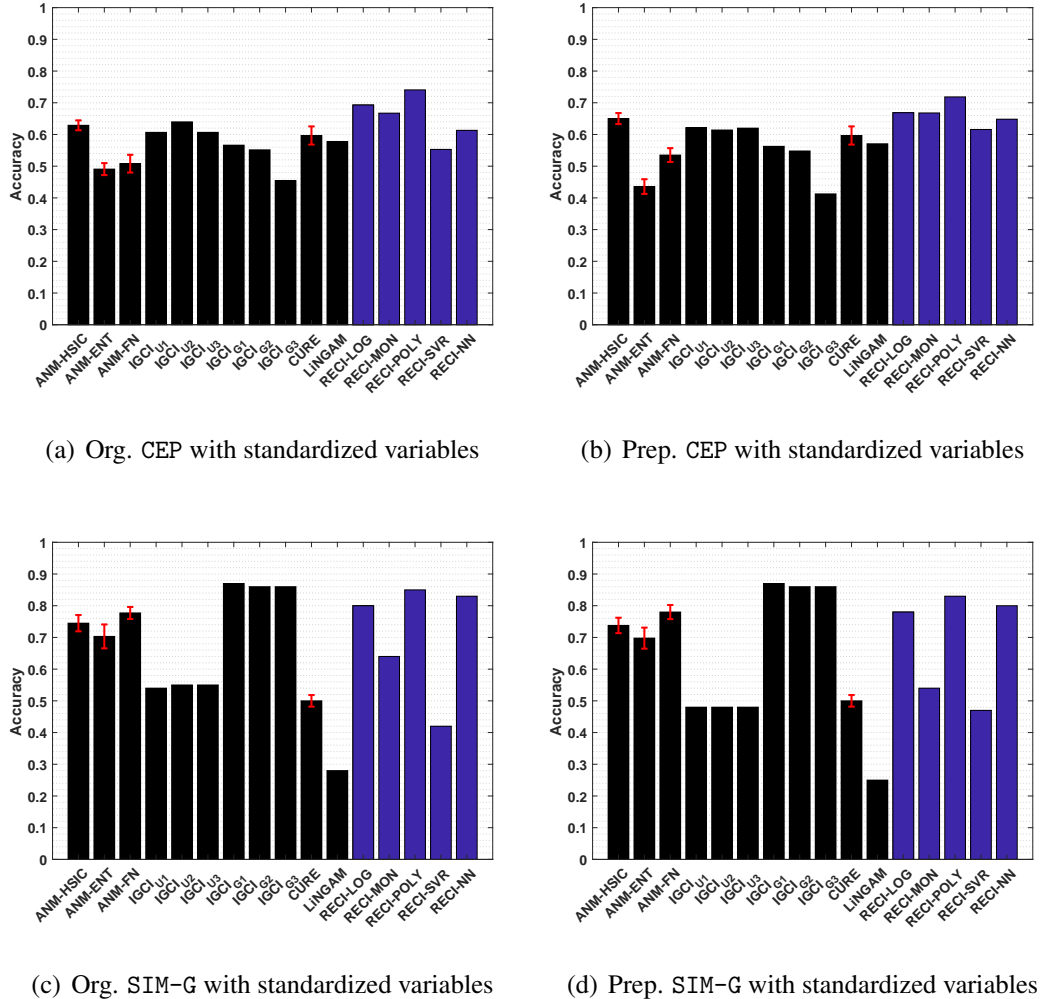


Figure 7: Evaluation result of all methods in the real-world CEP and SIM-G data sets. Here, a standardization instead of a normalization was used for the scaling in RECI. The figure on the left side shows the results of the evaluations in the original data and on the right side the results in the preprocessed versions where low-density points were removed.

D Tables

Table 7: The best performing parameters for each causal inference method in the artificial data sets Linear, Invertible and Non-invertible.

Data set	ANM estimator	IGCI configuration	RECI regression model
Linear	FN	IGCI _{U1}	MON: $ax^9 + c$
Invertible	HSIC	IGCI _{U2}	NN 4-8
Non-invertible	HSIC	IGCI _{U1}	POLY: $\sum_{i=0}^4 a_i x^i$

Table 2: The performances of all used classes of regression functions for RECI in the artificial and real-world benchmark data sets when averaging the MSE over all runs.

	CEP	Prep. CEP	SIM	Prep. SIM	SIM-c	Prep. SIM-c	SIM-1n	Prep. SIM-1n	SIM-G	Prep. SIM-G
LOG	68.93%	70.02%	61%	71%	70%	74%	72%	80%	72%	66%
$ax^2 + c$	72.13%	75.41%	43%	52%	57%	63%	44%	47%	44%	33%
$ax^3 + c$	72.27%	72.67%	45%	55%	58%	60%	45%	47%	43%	34%
$ax^4 + c$	71.58%	72.67%	50%	53%	56%	58%	45%	47%	43%	37%
$ax^5 + c$	69.92%	71.99%	51%	54%	60%	62%	44%	47%	45%	38%
$ax^6 + c$	68.84%	70.16%	52%	55%	61%	63%	42%	46%	45%	39%
$ax^7 + c$	67.75%	68.93%	52%	54%	62%	64%	42%	45%	47%	38%
$ax^8 + c$	67.61%	67.42%	51%	55%	62%	62%	41%	45%	44%	38%
$ax^9 + c$	66.56%	69.93%	50%	58%	63%	62%	42%	44%	45%	36%
$\sum_{i=0}^1 a_i x^i$	71.58%	66.51%	46%	54%	51%	58%	45%	43%	41%	26%
$\sum_{i=0}^2 a_i x^i$	70.09%	64.26%	53%	58%	65%	68%	69%	75%	54%	49%
$\sum_{i=0}^3 a_i x^i$	68.61%	64.49%	57%	63%	67%	71%	78%	76%	57%	52%
$\sum_{i=0}^4 a_i x^i$	66.63%	67%	57%	61%	68%	72%	80%	77%	60%	55%
$\sum_{i=0}^5 a_i x^i$	69.32%	66.54%	59%	63%	68%	71%	81%	75%	60%	53%
$\sum_{i=0}^6 a_i x^i$	67.32%	67%	60%	65%	68%	70%	82%	76%	64%	59%
$\sum_{i=0}^7 a_i x^i$	66.36%	67.55%	60%	65%	68%	72%	81%	74%	64%	58%
$\sum_{i=0}^8 a_i x^i$	68.87%	66.74%	60%	64%	68%	69%	82%	75%	65%	57%
$\sum_{i=0}^9 a_i x^i$	69.33%	66.74%	60%	64%	68%	69%	81%	74%	64%	55%
SVR	68.84%	66.51%	48%	54%	52%	59%	45%	43%	40%	26%
NN 2	65.87%	67%	57%	61%	68%	72%	81%	79%	60%	56%
NN 5	68.48%	65.85%	56%	59%	67%	70%	79%	76%	61%	56%
NN 10	64.82%	66.63%	57%	62%	68%	69%	80%	74%	62%	56%
NN 20	67.81%	70.53%	62%	63%	66%	70%	81%	72%	60%	57%
NN 2-4	64.28%	64.12%	55%	63%	68%	71%	78%	76%	60%	54%
NN 4-8	67.47%	65.85%	58%	62%	68%	68%	82%	76%	61%	55%

Table 3: The performances of all used classes of regression functions for RECI in the artificial and real-world benchmark data sets when not averaging the MSE.

	CEP	Pred. CEP	SIM	Prep. SIM	SIM-c	Prep. SIM-c	SIM-1n	Prep. SIM-1n	SIM-G	Prep. SIM-G
LOG	63.66% \pm 3.48	64.34% \pm 3.57	57.62% \pm 3.57	60.83% \pm 3.83	65.02% \pm 3.82	67.52% \pm 3.3	71.74% \pm 4.02	72.71% \pm 3.49	67.37% \pm 4.15	61.95% \pm 4.35
$ax^2 + c$	70.73% \pm 1.55	72.90% \pm 0.00	43.84% \pm 1.17	52% \pm 0.00	57% \pm 0.00	63% \pm 0.00	44.45% \pm 1.29	47% \pm 0.00	43.74% \pm 0.91	33.56% \pm 1.78
$ax^3 + c$	70.73% \pm 1.73	72.67% \pm 0.00	45.47% \pm 1.78	54% \pm 0.00	58% \pm 0.00	59% \pm 0.00	45.08% \pm 1.28	47.63% \pm 1.13	42.77% \pm 1.72	34.80% \pm 1.69
$ax^4 + c$	69.47% \pm 1.48	72.67% \pm 0.00	50% \pm 0.00	53% \pm 0.00	56.42% \pm 1.44	58.52% \pm 1.87	45% \pm 0.00	47% \pm 0.00	44.11% \pm 1.62	37.14% \pm 1.8
$ax^5 + c$	69.20% \pm 1.82	70.5% \pm 2.18	51% \pm 0.00	54% \pm 0.00	58.11% \pm 1.78	61% \pm 0.00	43.76% \pm 1.66	47% \pm 0.00	44.59% \pm 1.99	38.59% \pm 2.07
$ax^6 + c$	68.84% \pm 0.00	69.63% \pm 2.47	52% \pm 0.00	55% \pm 0.00	59% \pm 0.00	62.99% \pm 0.1	42.69% \pm 1.93	46% \pm 0.00	44% \pm 0.00	38.3% \pm 2.35
$ax^7 + c$	67.35% \pm 2.54	68.01% \pm 2.61	50% \pm 0.00	53.92% \pm 1.73	60% \pm 0.00	64% \pm 0.00	41.76% \pm 2.31	45% \pm 0.00	44% \pm 0.00	38% \pm 0.00
$ax^8 + c$	67.27% \pm 2.31	67.27% \pm 2.44	48.14% \pm 2.24	54.89% \pm 1.8	60.27% \pm 1.58	62% \pm 0.00	41% \pm 0.00	45% \pm 0.00	43.27% \pm 2.26	35% \pm 1.98
$ax^9 + c$	66.78% \pm 2.25	66.67% \pm 2.77	48.39% \pm 2.5	55.74% \pm 1.9	61% \pm 0.00	62% \pm 0.00	41% \pm 0.00	44% \pm 0.00	43% \pm 0.00	34.3% \pm 2.83
$\sum_{i=0}^1 a_i x^i$	68.84% \pm 0.00	66.28% \pm 0.00	45.77% \pm 1.54	54.37% \pm 1.47	51% \pm 0.00	58.24% \pm 1.62	45% \pm 0.00	43% \pm 0.00	41% \pm 0.00	26% \pm 0.00
$\sum_{i=0}^2 a_i x^i$	67.7% \pm 0.00	66% \pm 2.64	53.53% \pm 1.86	59.54% \pm 2.11	65% \pm 0.00	68% \pm 0.00	69% \pm 0.00	73% \pm 0.00	54.08% \pm 1.68	49% \pm 0.00
$\sum_{i=0}^3 a_i x^i$	67.24% \pm 0.00	65.4% \pm 1.97	57.67% \pm 2.4	61.43% \pm 2.58	67% \pm 0.00	70% \pm 0.00	78% \pm 0.00	75.54% \pm 1.22	57.26% \pm 1.95	52.01% \pm 2.31
$\sum_{i=0}^4 a_i x^i$	63.87% \pm 2.78	66.77% \pm 0.00	57.47% \pm 2.37	60.72% \pm 2.59	68% \pm 0.00	70% \pm 0.00	80% \pm 0.00	75.63% \pm 1.45	59.35% \pm 2.11	54% \pm 0.00
$\sum_{i=0}^5 a_i x^i$	64.85% \pm 0.00	66.54% \pm 0.00	57.3% \pm 2.72	61.79% \pm 2.12	68% \pm 0.00	70% \pm 0.00	81% \pm 0.00	75.49% \pm 1.56	59% \pm 0.00	53.06% \pm 2.37
$\sum_{i=0}^6 a_i x^i$	64.8% \pm 2.91	67% \pm 0.00	57.21% \pm 2.39	62.68% \pm 2.92	68% \pm 0.00	69% \pm 0.00	82% \pm 0.00	76% \pm 0.00	60.14% \pm 2.27	54.82% \pm 2.41
$\sum_{i=0}^7 a_i x^i$	65.08% \pm 0.00	67.55% \pm 0.00	62.5% \pm 2.92	68% \pm 0.00	69% \pm 0.00	81% \pm 0.00	74% \pm 0.00	60.04% \pm 2.29	55.15% \pm 2.89	
$\sum_{i=0}^8 a_i x^i$	65.39% \pm 0.00	66.74% \pm 0.00	60% \pm 0.00	62.06% \pm 2.86	68% \pm 0.00	82% \pm 0.00	75% \pm 0.00	61% \pm 0.00	55.84% \pm 3.06	
$\sum_{i=0}^9 a_i x^i$	65.39% \pm 0.00	66.74% \pm 0.00	58.01% \pm 2.82	62.15% \pm 2.82	68% \pm 0.00	69% \pm 0.00	81% \pm 0.00	74% \pm 0.00	60% \pm 0.00	55% \pm 0.00
SVR	66% \pm 0.38	64.67% \pm 2.73	46.12% \pm 1.79	54.33% \pm 2.06	52% \pm 0.00	59% \pm 0.00	41.37% \pm 2.1	43% \pm 0.00	40% \pm 0.00	25.69% \pm 1.88
NN 2	63.64% \pm 1.94	64.84% \pm 1.6	55.58% \pm 2.32	59.83% \pm 2.39	66.54% \pm 1.78	68.36% \pm 2	80.68% \pm 1.48	76.97% \pm 2.31	59.65% \pm 2.43	54.93% \pm 2.89
NN 5	63.92% \pm 2.06	65.69% \pm 1.52	56.69% \pm 2.56	58.66% \pm 2.51	66.49% \pm 0.97	68.26% \pm 2.28	79.72% \pm 1.74	74.58% \pm 3.17	60.26% \pm 2.53	54.67% \pm 3.11
NN 10	64.83% \pm 2.44	66.07% \pm 1.46	56.06% \pm 2.63	59.21% \pm 2.72	66.82% \pm 1.1	68.71% \pm 2.26	76.99% \pm 2.41	74.67% \pm 3.17	59.48% \pm 2.38	54.49% \pm 2.85
NN 20	64.9% \pm 3.02	66.87% \pm 2.19	58.69% \pm 2.62	59.72% \pm 3.23	66.36% \pm 2.78	69.46% \pm 2.42	76.36% \pm 2.84	73.10% \pm 2.83	58.98% \pm 2.9	54.83% \pm 3.21
NN 24	63.26% \pm 1.87	65.33% \pm 1.61	56.72% \pm 2.5	59.35% \pm 2.71	66.52% \pm 1.02	68.3% \pm 2.29	80.25% \pm 1.81	76.05% \pm 2.76	59.98% \pm 2.46	54.26% \pm 2.83
NN 48	64.33% \pm 2.23	66.05% \pm 1.44	56.33% \pm 2.53	58.84% \pm 2.71	66.48% \pm 1.77	68.5% \pm 2.59	78.71% \pm 2.01	73.31% \pm 2.6	59.76% \pm 2.51	55.44% \pm 2.61

Table 4: The performances of all used classes of regression functions for RECI in the standardized CEP and SIM-G data sets when averaging the MSE over all runs.

	Standardized CEP	Standardized Prep. CEP	Standardized SIM-G	Standardized Prep. SIM-G
LOG	69.29%	66.87%	80%	78%
$ax^2 + c$	63.57%	61.59%	38%	34%
$ax^3 + c$	61.99%	64.71%	60%	47%
$ax^4 + c$	65.44%	66.79%	40%	23%
$ax^5 + c$	64.61%	62.71%	63%	48%
$ax^6 + c$	65.65%	65.72%	56%	43%
$ax^7 + c$	64.49%	64.26%	63%	47%
$ax^8 + c$	66.72%	65.76%	61%	54%
$ax^9 + c$	65.86%	65.84%	64%	51%
$\sum_{i=0}^1 a_i x^i$	60.83%	61.25%	50%	49%
$\sum_{i=0}^2 a_i x^i$	74.07%	63.99%	83%	83%
$\sum_{i=0}^3 a_i x^i$	67.47%	66.01%	83%	83%
$\sum_{i=0}^4 a_i x^i$	69.27%	66.07%	85%	83%
$\sum_{i=0}^5 a_i x^i$	69.54%	66.95%	85%	82%
$\sum_{i=0}^6 a_i x^i$	72.94%	71.85%	83%	81%
$\sum_{i=0}^7 a_i x^i$	67.30%	71.19%	83%	82%
$\sum_{i=0}^8 a_i x^i$	67.87%	65.70%	83%	82%
$\sum_{i=0}^9 a_i x^i$	68.89%	68.31%	81%	81%
SVR	55.30%	61.58%	42%	47%
NN 2	55.19%	64.82%	80%	78%
NN 5	56.85%	61.35%	81%	76%
NN 10	60.57%	58.90%	80%	80%
NN 20	56.75%	60.89%	79%	79%
NN 2-4	60.09%	57.78%	72%	77%
NN 4-8	59.13%	59.21%	80%	80%

Table 5: The performances of all used classes of regression functions for RECI in the standardized CEP and SIM-G data sets when not averaging the MSE.

	Standardized CEP	Standardized Prep. CEP	Standardized SIM-G	Standardized Prep. SIM-G
LOG	53.86% \pm 5.33	54.18% \pm 6.12	76.67% \pm 3.26	76.21% \pm 3.13
$ax^2 + c$	62.41% \pm 0.00	61.59% \pm 0.00	40.83% \pm 4.77	39.79% \pm 3.67
$ax^3 + c$	61.99% \pm 0.00	60.81% \pm 0.05	54.42% \pm 3.53	47.91% \pm 4.12
$ax^4 + c$	65.44% \pm 0.00	66.79% \pm 0.00	37.10% \pm 3.34	29.85% \pm 3.90
$ax^5 + c$	56.80% \pm 0.00	58.79% \pm 0.02	57% \pm 0.00	45.33% \pm 4.81
$ax^6 + c$	65.65% \pm 0.00	64.18% \pm 0.00	45% \pm 0.00	35.60% \pm 3.80
$ax^7 + c$	60.53% \pm 0.00	57.39% \pm 0.00	53% \pm 0.00	44.65% \pm 4.10
$ax^8 + c$	65.73% \pm 0.63	62.91% \pm 0.00	50.37% \pm 3.76	41.36% \pm 5.09
$ax^9 + c$	63.72% \pm 0.92	58.79% \pm 0.00	53% \pm 0.00	50% \pm 0.00
$\sum_{i=0}^1 a_i x^i$	56.05% \pm 5.73	57.78% \pm 6.10	54% \pm 0.00	50.01% \pm 4.17
$\sum_{i=0}^2 a_i x^i$	60.03% \pm 5.66	59.82% \pm 0.00	83% \pm 0.00	83% \pm 0.00
$\sum_{i=0}^3 a_i x^i$	60.52% \pm 0.00	59.14% \pm 4.47	83% \pm 0.00	83% \pm 0.00
$\sum_{i=0}^4 a_i x^i$	61.04% \pm 4.80	61.14% \pm 4.65	83% \pm 0.00	83% \pm 0.00
$\sum_{i=0}^5 a_i x^i$	62.03% \pm 0.00	62.07% \pm 4.54	81% \pm 0.00	81% \pm 0.00
$\sum_{i=0}^6 a_i x^i$	61.45% \pm 4.99	62.28% \pm 4.87	80% \pm 0.00	80% \pm 0.00
$\sum_{i=0}^7 a_i x^i$	61.45% \pm 4.02	63.36% \pm 4.56	83% \pm 0.00	82% \pm 0.00
$\sum_{i=0}^8 a_i x^i$	62.37% \pm 5.10	63.35% \pm 4.20	83% \pm 0.00	82% \pm 0.00
$\sum_{i=0}^9 a_i x^i$	63.70% \pm 4.53	63.27% \pm 4.16	81% \pm 0.00	81% \pm 0.00
SVR	55.12% \pm 5.50	57.15% \pm 5.49	46.69% \pm 4.65	47% \pm 0.00
NN 2	55.89% \pm 5.30	57.12% \pm 5.70	80.07% \pm 2.38	80.04% \pm 2.74
NN 5	55.61% \pm 5.87	57.31% \pm 6.08	78.10% \pm 2.23	77.29% \pm 2.35
NN 10	56.63% \pm 5.37	57.08% \pm 3.52	76.68% \pm 2.41	77.10% \pm 2.50
NN 20	55.93% \pm 6.55	58.07% \pm 5.76	75.45% \pm 2.76	75.78% \pm 2.94
NN 2-4	56.26% \pm 6.47	56.27% \pm 6.03	78.71% \pm 2.69	78.26% \pm 2.62
NN 4-8	56.57% \pm 3.70	57.65% \pm 3.47	77.04% \pm 2.19	77.60% \pm 2.40

Table 6: All performances of ANM, IGCI, CURE and LiNGAM.

	CEP	Prep. CEP		SIM		Prep. SIM		SIM-c		Prep. SIM-c		SIM-1n		Prep. SIM-1n		SIM-G		Prep. SIM-G	
		62.89% \pm 1.56	65.01% \pm 1.74	75.54% \pm 2.14	73.33% \pm 2.08	80.54% \pm 2.14	77.93% \pm 2.02	76.60% \pm 2.53	70.98% \pm 2.40	74.49% \pm 2.40	74.49% \pm 2.57	73.78% \pm 2.44							
ANM-HSIC	49.07% \pm 1.88	43.57% \pm 2.31	72.91% \pm 3.09	71.51% \pm 3.35	76.36% \pm 3.14	74.95% \pm 3.57	78.88% \pm 2.63	73.93% \pm 2.88	70.32% \pm 3.77	70.32% \pm 3.77	69.78% \pm 3.32								
ANM-ENT	50.80% \pm 2.80	53.50% \pm 2.18	57.50% \pm 1.60	51.94% \pm 1.92	61.15% \pm 1.99	59.57% \pm 1.93	85.31% \pm 1.36	80.03% \pm 1.31	77.72% \pm 1.90	77.72% \pm 1.90	78% \pm 2.23								
ANM-FN	60.66% \pm 0.90	62.13% \pm 0.90	36% \pm 0.00	39% \pm 0.00	46% \pm 0.00	47% \pm 0.00	51% \pm 0.00	57% \pm 0.00	54% \pm 0.00	54% \pm 0.00	48% \pm 0.00								
IGCI _{U,1}	63.97% \pm 0.00	61.40% \pm 0.00	41% \pm 0.00	42% \pm 0.00	50% \pm 0.00	52% \pm 0.00	52% \pm 0.00	57% \pm 0.00	55% \pm 0.00	55% \pm 0.00	48% \pm 0.00								
IGCI _{U,2}	60.67% \pm 0.00	61.99% \pm 0.00	41% \pm 0.00	42% \pm 0.00	50% \pm 0.00	52% \pm 0.00	52% \pm 0.00	57% \pm 0.00	55% \pm 0.00	55% \pm 0.00	48% \pm 0.00								
IGCI _{U,3}	56.62% \pm 0.00	56.26% \pm 0.00	36% \pm 0.00	36% \pm 0.00	42% \pm 0.00	41% \pm 0.00	42% \pm 0.00	59% \pm 0.00	57% \pm 0.00	87% \pm 0.00	87% \pm 0.00								
IGCI _{G,1}	55.15% \pm 0.00	54.79% \pm 0.00	37% \pm 0.00	38% \pm 0.00	46% \pm 0.00	45% \pm 0.00	61% \pm 0.00	60% \pm 0.00	86% \pm 0.00	86% \pm 0.00	86% \pm 0.00								
IGCI _{G,2}	45.45% \pm 0.00	41.26% \pm 0.00	37% \pm 0.00	38% \pm 0.00	46% \pm 0.00	45% \pm 0.00	61% \pm 0.00	60% \pm 0.00	86% \pm 0.00	86% \pm 0.00	86% \pm 0.00								
IGCI _{G,3}	59.67% \pm 2.86	59.67% \pm 2.86	59.62% \pm 3.30	59.62% \pm 3.30	68.60% \pm 3.68	68.60% \pm 3.68	55.58% \pm 1.82	55.58% \pm 1.82	47.46% \pm 0.96	47.46% \pm 0.96	47.46% \pm 0.96								
CURE	57.76% \pm 0.00	57.06% \pm 0.00	43% \pm 0.00	49% \pm 0.00	47% \pm 0.00	52% \pm 0.00	24% \pm 0.00	25% \pm 0.00	28% \pm 0.00	28% \pm 0.00	25% \pm 0.00								
LiNGAM																			

E Plots

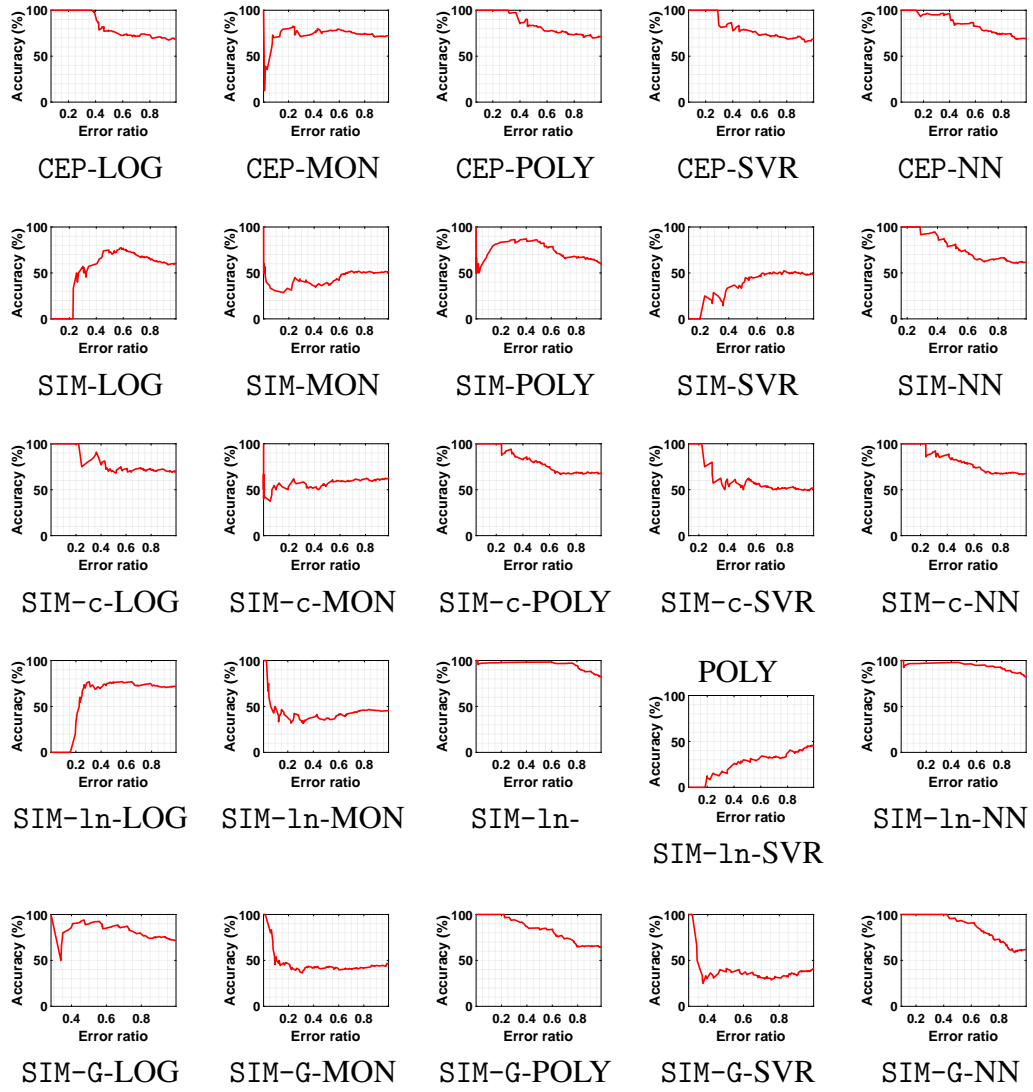


Figure 8: The performance of RECI in the original data sets with respect to the error ratio (10) as rejection criterion.

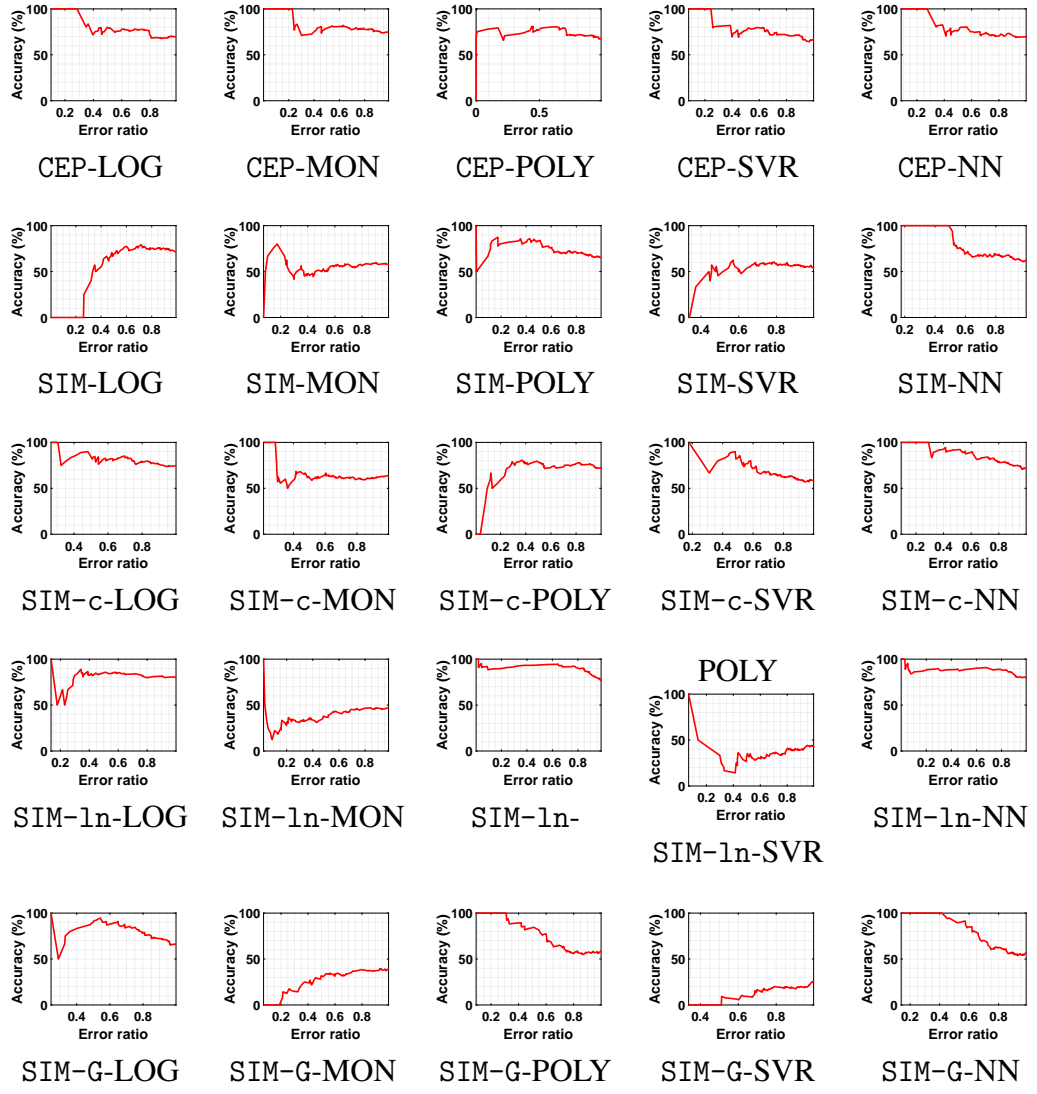


Figure 9: The performance of RECI in the preprocessed data sets with respect to the error ratio (10) as rejection criterion.

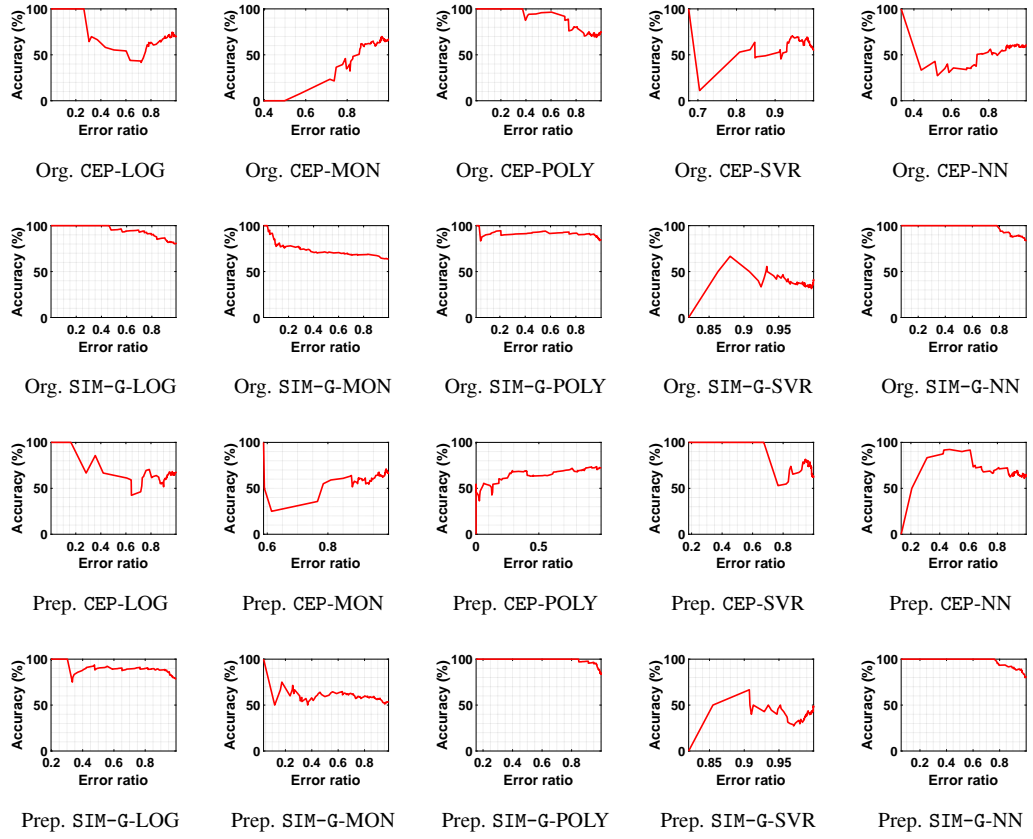


Figure 10: The performance of RECI in the standardized data sets with respect to the error ratio (10) as rejection criterion.

References

- [1] P. Blöbaum, D. Janzing, T. Washio, S. Shimizu, and B. Schölkopf. Cause-effect inference by comparing regression errors. In *Proceedings of the 21st International Conference on Artificial Intelligence and Statistics (AISTATS 2018)*, 2018.
- [2] J. Pearl. *Causality: Models, Reasoning and Inference*. Cambridge University Press, New York, NY, USA, 2nd edition, 2009.
- [3] P. Spirtes, C. Glymour, and R. Scheines. *Causation, prediction, and search*. MIT press, 2000.
- [4] J. Peters, D. Janzing, and B. Schölkopf. *Elements of Causal Inference – Foundations and Learning Algorithms*. MIT Press, 2017. <http://www.math.ku.dk/~peters/>.
- [5] Y. Kano and S. Shimizu. Causal inference using nonnormality. In *Proceedings of the International Symposium on Science of Modeling, the 30th Anniversary of the Information Criterion*, pages 261–270, Tokyo, Japan, 2003.
- [6] J. W. Comley and D. L. Dowe. General Bayesian networks and asymmetric languages. In *Proceedings of the Second Hawaii International Conference on Statistics and Related fields*, June 2003.
- [7] S. Shimizu, P. Hoyer, A. Hyvärinen, and A. Kerminen. A linear non-Gaussian acyclic model for causal discovery. *Journal of Machine Learning Research*, 7:2003–2030, 2006.
- [8] X. Sun, D. Janzing, and B. Schölkopf. Causal inference by choosing graphs with most plausible Markov kernels. In *Proceedings of the 9th International Symposium on Artificial Intelligence and Mathematics*, pages 1–11, Fort Lauderdale, FL, 2006.
- [9] K. Zhang and A. Hyvärinen. On the identifiability of the post-nonlinear causal model. In *Proceedings of the 25th Conference on Uncertainty in Artificial Intelligence*, pages 647–655, Arlington, Virginia, United States, June 2009. AUAI Press.
- [10] P. Hoyer, D. Janzing, J. Mooij, J. Peters, and B. Schölkopf. Nonlinear causal discovery with additive noise models. In *Advances in Neural Information*

Processing Systems 21, pages 689–696, Red Hook, NY, USA, June 2009. Curran Associates, Inc.

- [11] D. Janzing, X. Sun, and B. Schölkopf. Distinguishing cause and effect via second order exponential models. eprint <http://arxiv.org/abs/0910.5561>, 2009.
- [12] J. Peters, D. Janzing, and B. Schölkopf. Causal inference on discrete data using additive noise models. *IEEE Transactions on Pattern Analysis and Machine Intelligence*, 33(12):2436–2450, 2011.
- [13] P. Daniušis, D. Janzing, J. Mooij, J. Zscheischler, B. Steudel, K. Zhang, and B. Schölkopf. Inferring deterministic causal relations. In *Proceedings of the 26th Conference on Uncertainty in Artificial Intelligence*, pages 143–150, Corvallis, OR, USA, July 2010. AUAI Press.
- [14] D. Janzing, J. Mooij, K. Zhang, J. Lemeire, J. Zscheischler, P. Daniušis, B. Steudel, and B. Schölkopf. Information-geometric approach to inferring causal directions. *Artificial Intelligence*, 182:1–31, May 2012.
- [15] E. Sgouritsa, D. Janzing, P. Hennig, and B. Schölkopf. Inference of cause and effect with unsupervised inverse regression. In *Artificial Intelligence and Statistics*, pages 847–855, 2015.
- [16] J. Mooij, Peters J., D. Janzing, J. Zscheischler, and B. Schölkopf. Distinguishing cause from effect using observational data: Methods and benchmarks. *Journal of Machine Learning Research*, 17(32):1–102, January 2016.
- [17] D. Janzing and B. Schölkopf. Causal inference using the algorithmic Markov condition. *IEEE Transactions on Information Theory*, 56(10):5168–5194, 2010.
- [18] J. Lemeire and D. Janzing. Replacing causal faithfulness with algorithmic independence of conditionals. *Minds and Machines*, 23(2):227–249, 7 2012.
- [19] B. Schölkopf, D. Janzing, J. Peters, E. Sgouritsa, K. Zhang, and J. Mooij. *Semi-supervised learning in causal and anticausal settings*, chapter 13, pages 129–141. Festschrift in Honor of Vladimir Vapnik. Springer-Verlag, 2013.

- [20] P. Blöbaum, T. Washio, and S. Shimizu. Error asymmetry in causal and anticausal regression. *Behaviormetrika*, pages 1–22, 2017.
- [21] P. Blöbaum, S. Shimizu, and T. Washio. A novel principle for causal inference in data with small error variance. In *ESANN*, 2017.
- [22] A. Hyvärinen and S. Smith. Pairwise likelihood ratios for estimation of non-gaussian structural equation models. *Journal of Machine Learning Research*, 14(Jan):111–152, 2013.